2015

Modeling Uric Acid Kidney Stones Disease in D. melanogaster using RNAi and Dietary Modulation

https://doi.org/10.33015/dominican.edu/2015.bio.05

Hai T.H. Lu
Dominican University of California

Modeling Uric Acid Kidney Stones Disease in *D. melanogaster* using RNAi and Dietary Modulation

a thesis submitted to faculty of Dominican University of California

and the Buck Institute for Research on Aging

in partial fulfillment of the requirements

For the degree

Master of Science

in

Biology

By

Hai Lu

San Rafael, California

2014

Certification of Approval

I certify that I have read Modeling Uric Acid Kidney Stones Disease in *D. melanogaster* using RNAi and Dietary Modulation

By Hai Lu,

and I approved this thesis to be submitted in partial fulfillment of the requirements for the degree: Master of Sciences in Biology at Dominican University of California & the Buck Institute for Research on Ageing.

_____

Dr. Pankaj Kapahi, PhD

Graduate Research Advisor

Professor at the Buck Institute for Research on Ageing

_____

Dr. Roland Cooper, PhD

Professor at Dominican University of California

_____

Dr. Maggie Louie, PhD

Dominican University of California Graduate Program Director

This page is left blank intentionally.

Abstract

In humans, the major predictor for gout and forming uric acid kidney stones is elevated uric acid in the serum and urine respectively. It is known that uric acid is an end metabolite of purine degradation in humans, but in other species from *D. melanogaster* to lower apes, uric acid can be further metabolized by urate oxidase into readily excreted allantoin. We hypothesize that if urate oxidase enzyme activity and dietary purine are both critical in uric acid kidney stone formation, then urate oxidase knockdown in combination with dietary purine supplementation will increase uric acid and induce uric acid kidney stone formation in *D. melanogaster*. Initially, we confirmed urate oxidase knockdown and then elevation of uric acid as a consequence. We then confirmed uric acid kidney stones formed as a consequence of urate oxidase knocked down and a high purine diet. Next, we tested compounds used to treat gout or uric acid kidney stones in humans using our model. We found that allopurinol and potassium citrate reduced uric acid kidney stone formation in our model. We then tested whether compounds predicted to reduce uric acid and uric acid kidney stones in humans, but not currently used as treatments, can reduce uric acid kidney stone formation in our model. We found that methotrexate, hydrochlorothiazide, and l-lysine were effective at reducing uric acid kidney stone formation. Lastly, we ran a medium throughput screen of 117 natural compounds for inhibitors of uric acid kidney stone formation using our model and found seven inhibitors.

Acknowledgments

First, I would like to acknowledge the great effort and tireless dedication of my advisor: Dr. Pankaj Kapahi and post-doctoral mentor: Dr. Sven Lang. They have both been intricately involved in my development and growth as a scientist and their guidance has been truly invaluable to my personal and intellectual development. The entirety of all that I have learned can be eloquently summed up in the timeless words of Albert Einstein, "One thing I have learned in a long life: that all our science, measured against reality, is primitive and childlike and yet it is the most precious thing we have."

Secondly, I would like to also take the time to acknowledge Dr. Roland Cooper for graciously offering his time to serve as the second reader for my Master's thesis.

Lastly, I dedicated this thesis and poem to my mother. The support and love you have provided me over the years cannot be repaid with gifts or worldly things, but I hope this poem can show you how much you are appreciated.

Poem written by Ngô Xuân Hậu

Cho Mẹ sao ngủ trên trời

Trăng du đáy nước rừng mời dấu chân

Cho mẹ giọng hát thiên thần Sóng xô tiếng nhạc mỗi lần mẹ ru

Cho mẹ miền ấy sang thu Gío lay lá gọi sương mù bao quanh

Cho mẹ mùa ấy thanh bình

Ôm con với mộng đăng trình trong tay

Table of Contents

1 List of Figures

2 List of Tables

3 Abbreviations

GS
: Gene Switch

HCT
: Hydrochlorothiazide

HP
: High Purine

L-Lys
: L-Lysine

LP
: Low purine

MTX
: Methotrexate

RNAi
: RNA Interference

UO
: Urate Oxidase

UA
: Uric Acid

XDH
: Xanthine Dehydrogenase

XO
: Xanthine Oxidase

4 Introduction

No class of molecule consistently reappears in the large number of different biological processes as purines, making them the most widely found alkaloid or nitrogen containing heterocyclic compound in nature (Rosemeyer, 2004). Purines are components of molecules that are essential to many cellular processes like DNA replication, transcription, translation, and energy metabolism. Without purines, these essential processes could not occur and life could not exist as we know it. Because purine structures are important to a large number of different biological processes; purine *de novo* synthesis, salvage, degradation, and excretion is tightly regulated across species ranging from humans to bacteria (Boss and Seegmiller, 1982; Gots et al., 2009; Jurecka, 2009; Mandal et al., 2003; Mendz et al., 1997; Nudler and Mironov, 2004).

Disorders of purine degradation like gout and uric acid kidney stones have been well documented in western literature since Greek times. In the Hippocratic Corpus written sometime between 420-370 BC, the Greeks refer to gout by the word *podagra*, which literately means “the un-walkable disease” (Singer and Underwood, 1962). The most common symptoms were painful swelling and acute inflammation and arthritis of the first toe in the first metatarsophalangeal joint, which can cause crippling loss of mobility, giving gout its Greek namesake. The Hippocratic Oath indirectly mentions surgeons that specifically performed lithotomies, the removal of stones from the body, a large number of which were uric acid kidney stones (Edelstein, 1943). Patients with uric acid kidney stones or kidney stones in general experience reoccurring episodes of extreme and severe pain that begins from the flanks or lower back of their abdomen and progresses to the inner thigh or groin area that are called renal colic pain (Preminger, 2007). Renal colic pain has been described as one of the strongest pain sensations

known in the human experience and is accompanied by a host of acute symptoms like nausea and vomiting to name only a few (Wolf, 2014). To understand gout and uric acid kidney stones, diseases that have both been with humans since time in memorial, we need to examine how purines are degraded and how they are eliminated.

4.1 Purine Structure

A purine is a conjugated heterocyclic organic compound containing a pyrimidine ring fused with an imidazole ring. The pyrimidine is a six member coplanar ring containing two nitrogen atoms (Fig. 1). The imidazole ring is also coplanar and consists of a five member ring containing two nitrogen atoms (Fig. 1). Different types of purines like adenine and guanine bases can be created by substituting different functional groups on the ring structure (Fig. 1). Pyrimidines and purines are both nitrogenous bases that are structural components of nucleosides and nucleotides. Nucleosides are pyrimidine or purine nitrogenous bases attached to a ribose sugar at the 1' carbon atom of the sugar molecule. Nucleotides are nucleoside structures with a phosphate group attached to the 5' carbon atom of the sugar.

4.2 Purines in cellular metabolism

Adenine has a primary amine group ($-NH_2$) attached at carbon 6 of the purine ring while guanine has oxygen double bonded at the same carbon and a primary amine group attached at carbon 2 (Fig. 2). Purine (adenine and guanine) deoxyribonucleotides form hydrogen bonds complementary to pyrimidine (thymine and cytosine) deoxyribonucleotides in a DNA double helix. Information is stored in the sequence of purines and pyrimidine bases. With this genetic

code, information contained in the DNA sequence can be replicated using one or both strands of DNA. In the production of pre-mRNA, pyrimidine ribonucleotides are inserted complementary to purine deoxyribonucleotides and vice versa. This pre-mRNA strand is processed and exons are spliced together while the introns are excluded and degraded. The final mRNA sequence of adenine, guanine, uracil, and cytosine ribonucleotides is produced. The mRNA sequence is used as template for translation by the ribosome to synthesize the encoded polypeptide or protein. Without adenine and guanine bases, replication, transcription, and translation all could not occur as individual steps or together.

4.3 Purines in energy metabolism

Adenosine diphosphate (ADP) is also a component of various key molecules that are involved in energy metabolism like adenine triphosphate (ATP), nicotinamide adenine dinucleotide phosphate (NADPH), nicotinamide adenine dinucleotide (NAD), flavin adenine dinucleotide (FAD), and Coenzyme A (CoA). For example, ATP is composed of a ribose sugar with adenine attached to the 1' carbon atom and three phosphate groups attached to the 5' carbon atom (Fig. 3). ATP serves as the main molecular battery that stores usable energy for the cell. Chemical energy is stored between the bond of the β and γ-phosphate groups (anhydride bonds) and this chemical energy is used during enzyme-catalyzed hydrolysis or phosphorylation to power such processes as DNA and protein synthesis (Nelson and Cox, 2000). During the elongation phase of DNA synthesis, DNA polymerase extends an existing DNA strand by adding nucleotides complementary to a template strand and forming phosphodiester bonds between the 3' hydroxyl group of the existing strand and 5' phosphate group of the newly incorporated nucleotide (Nelson and Cox, 2000). Elongation occurs uninterrupted to the leading strand of

DNA, but the lagging strand must have their Okazaki fragments ligated together by DNA ligase, which requires ATP (Nelson and Cox, 2000). Without ATP, DNA replication would be incomplete. During translation, the production of aminoacyl-tRNA requires the initial reaction between the α-carboxyl of an amino acid with the α-phosphate of an ATP molecule to form a 5' amino-acyl adenylate (Nelson and Cox, 2000). Without ATP, aminoacyl-tRNAs would be unavailable for protein synthesis. Energy contained in the structure of ATP is essential for both DNA replication and protein synthesis to name only a few biological processes.

NADH is a triphosphate dinucleotide that is an extremely important cofactor involved in many catabolic cellular processes. One nucleotide consists of a ribose sugar phosphorylated at the 5' carbon atom and adenine attached to the 1' carbon atom. The second nucleotide consists of another ribose sugar phosphorylated at the 5' carbon atom and nicotinamide attached to the 1' carbon atom. The two nucleotides are attached via a diphosphate bond between the 5' carbons of the two ribose sugars to form NADH (Fig. 4). In cellular metabolism, NAD^+ accepts electrons and NADH (the reduced form) donates electrons in redox reactions (Belenky et al., 2007). Redox reactions in catabolic pathways like beta oxidation, citric acid cycle, and glycolysis reduce NAD^+ to NADH (Nelson and Cox, 2000). NADH can then act as a reducing agent and cofactor in an anabolic process like gluconeogenesis (Sistare and Haynes, 1985). Without ATP or NADH, energy metabolism would be severely compromised and essential cellular processes would cease.

4.4 Purine metabolism in humans and *D. melanogaster*

Purines are made available through either dietary intake (Bauer et al., 2006; Choi et al., 2005), constructed *de novo* using intracellular components to form the purine ring, or recycled via a salvage pathway (Kanehisa and Goto, 2000; Nelson and Cox, 2000). In both species, a

dramatic change in the quantity of purines made available by one pathway can be compensated for by modulating the other pathways accordingly. However, the elimination of purines has no such natural compensatory mechanism for both species. The elimination of adenine and guanine or its nucleotide derivatives converge downstream at xanthine (Kanehisa and Goto, 2000; Nelson and Cox, 2000). There are no enzymatic catalyzed alternative routes for purine elimination that bypasses xanthine for either species (Kanehisa and Goto, 2000; Nelson and Cox, 2000).

4.5 Purine degradation pathway to xanthine in humans and *D. melanogaster*

Xanthine consists of a purine ring with oxygen double bonded to a carbon at position 2 and 6 of the purine ring (Fig. 5). As shown in Fig. 6, xanthine can be created from the degradation of adenine, guanine, or inosine nucleotides in humans and *D. melanogaster* (KG: 230)(Kanehisa and Goto, 2000). In both species, adenine monophosphate is first converted into adenosine by 5'nucleotidase (KG:3.1.3.5)(Kanehisa and Goto, 2000). Adenosine is then converted into inosine by adenosine deaminase and inosine is converted into hypoxanthine (the oxidized form of xanthine) by nucleosidase (KG:3.5.4.4)(Kanehisa and Goto, 2000). Xanthine oxidase (XO), a form of xanthine oxidoreductase, finally converts hypoxanthine into xanthine (KG:1.17.3.2 & 1.17.1.4)(Kanehisa and Goto, 2000). To degrade guanine nucleotides, guanine monophosphate nucleotide is first converted into guanosine by 5'nucleotidase (KG:3.1.3.5)(Kanehisa and Goto, 2000). Guanosine is then converted into guanine by nucleosidase (KEGG: 2.4.2.1)(Kanehisa and Goto, 2000). Finally, guanine is converted into xanthine by guanine deaminase (KG:3.5.4.3)(Kanehisa and Goto, 2000).

4.6 Degradation of xanthine to uric acid and urate in humans and *D. melanogaster*

In both humans and *D. melanogaster*, xanthine is converted into uric acid (UA) by xanthine oxidase (Fig. 6)(KG:1.17.3.2 1.17.1.4)(Kanehisa and Goto, 2000; Nelson and Cox, 2000). Xanthine can also be directly converted into urate (the ionic form of uric acid) by xanthine dehydrogenase (XDH), another form of xanthine oxidoreductase (Eger et al., 2000; Enroth et al., 2000). Uric acid consists of a purine ring with 3 oxygen atoms double bonded to carbon atoms at position 2, 6, and 8 (Fig. 7). Uric acid is a diprotic acid with a $pKa_1 = 5.7$ and $pKa_2 = 10.3$ with a solubility constant of 7 mg/dL at 25 °C (McCrudden, 2008). Uric acid can reversibly form a singly charged urate anion ion (Fig. 7) that can conjugate with a base anion to form a urate salt. At physiological pH, monosodium urate is the predominate salt and is nearly 50 times more abundant and more soluble than uric acid (Liebman et al., 2007). When pH decreases, more insoluble uric acid forms rather than the more soluble urate salts. In summary, every major step of purine degradation from the major nucleotide metabolites to uric acid and urate is conserved when comparing humans and *D. melanogaster*.

4.7 Uric acid elimination in humans

Xanthine oxidoreductase is expressed in almost every type of human cell, tissue, and organ from serum (blood) to lung, with the highest levels of expression occurring in the cerebellum, skeletal muscle, liver, bone marrow, heart, and kidney (Sarnesto et al., 1996). Urate can therefore be ubiquitously produced in humans from almost all cells, tissues and organs with the largest amount being produced by the liver, muscles and intestine (Hediger et al., 2005). Urate can also be produced by xanthine dehydrogenase in the serum. Once in the circulatory system, urate is delivered to the glomerulus where it freely passes and enters the renal system.

The nephritic filtrate that is produced then travels down the proximal convoluted tubule where URAT1 (*SLC22A12*), OAT1/OAT3 (*SLC22A11*), and OAT4/OAT10 (*SLC22A13*) transporter proteins reabsorb roughly 90 percent of the urate back into the circulatory system (Enomoto et al., 2002; Terkeltaub et al., 2006). The remaining urate that is not reabsorbed will eventually be excreted in urine.

In many other species, from flies to lower apes, urate oxidase (UO) can metabolize uric acid into allantoin (Nelson and Cox, 2000). Allantoin is a uric acid molecule with the bond between carbon 4 and nitrogen 3 oxidized losing the typical purine ring structure (Fig. 8). Allantoin is nearly an order of magnitude more soluble than urate with a solubility constant of 57 mg/dl at 25 °C (Yalkowsky and He, 2003). Humans lost the ability to convert uric acid into allantoin at some point during the Miocene epoch between 8 to 20 million years ago due to sequential mutations to the promoter and then to the coding region of *urate oxidase* (Oda et al., 2002). Thus, the *urate oxidase* gene is a so-called pseudogene in humans that is not expressed (Kratzer et al., 2014).

4.8 Gout and uric acid kidney stones in humans

Because of the low solubility of uric acid (7 mg/dL at 25 °C), uric acid can precipitate out of body fluids like serum or urine to form mineralized concretions. This can initiate gout and uric acid kidney stones respectively. Gout is an inflammatory disease characterized by elevated uric acid levels in the blood (hyperuricemia) that leads to deposition of monosodium urate crystals within joints and eventually acute arthritis in patients (Wortmann and Kelley, 2005). Patients with hyperuricemia are statistically more likely to develop gout (Choi et al., 2005; McGill and Dieppe, 1991). A urate serum level greater than 7.0 mg/dl for extended periods of time is the

primary risk factor for developing gout (Campion et al., 1987). Around 8.3 million or around 3% of population in the United States will develop gout at some point in their life (Zhu et al., 2011). To prevent gout, a large component of the treatment effort focuses on lowering uric acid and urate levels in the serum. Non-drug treatments to lower serum urate include reducing sodium intake, reducing intake of purine rich foods, staying hydrated, losing weight if overweight, decreasing alcohol intake, and regular exercise (Choi et al., 2005; Frassetto and Kohlstadt, 2011). Drug treatments include nonsteroidal anti-inflammatory drugs, colchicines, and steroids (Nelson and Cox, 2000), as well as probenecid (Sriranganathan et al., 2014), allopurinol (Akkasilpa et al., 2004; Sriranganathan et al., 2014), and febuxostat (Schlesinger, 2010).

People with serum urate levels greater than 7.0 mg/dl are also more likely to develop uric acid kidney stones (Wortmann and Kelley, 2005). Uric acid kidney stones are crystalline concretions that form in the kidney or urinary track from precipitation and aggregation of uric acid or urate in urine. The uric acid kidney stones can obstruct the urinary tract which causes excruciating renal colic pain to patients. Two major predictors of forming uric acid kidney stones in humans are urine pH and uric acid concentration in serum and urine (Dardamanis, 2013). In the United States, kidney stones occurs in 6-12% of the general population (Stamatelou et al., 2003). Of this 6-12% of people who experience kidney stones, 5-10% of them experience uric acid kidney stones (Bushinsky, 2001), but rates of uric acid kidney stones can reach as high as 37.7% in the general population in other parts of the world like Iran (Halabe and Sperling, 1994). The probability of forming uric acid kidney stones after the first episode increases by 23% and each subsequent episode further increases the likelihood of uric acid kidney stone formation (Trinchieri et al., 1999b). To prevent uric acid kidney stones, major effort is made to lower uric acid and urate concentrations in the serum and urine of patients using pH alkalizing compounds

such as potassium citrate (Maalouf, 2014; Sorkhi et al., 2011). Non drug treatments to reduce serum uric acid and urate levels include reducing the intake of sodium, reducing the intake of purine rich foods, staying hydrated, losing weight if overweight, decreasing alcohol intake, and regular exercise (Choi et al., 2005), which are some of the same treatments recommended to gout patients. Drug treatments available for uric acid kidney stones are benzbromarone (Akkasilpa et al., 2004), and allopurinol (Halabe and Sperling, 1994).

4.9 *D. melanogaster* is a robust model organism for developing a model of uric acid kidney stone disease

Is *D. melanogaster* well suited for our endeavor? The genome of *D. melanogaster* is relatively small at 180 Mpb (vs. humans ~ 3,000 Mbp), composed of one pair of sex chromosome (the first chromosome pair) and three pairs of autosomes (the second, third, and fourth chromosome pair respectively) for a total of four chromosome pairs (Henderson, 2004). Additionally, *Drosophila* genetics follow traditional Mendelian patterns of inheritance and can easily be bred to produce flies of a desired genotype and phenotype (Henderson, 2004). Thus, flies offer a great system in which genetic manipulation can be performed to induce uric acid kidney stone formation.

Insects like *D. melanogaster* do not possess a vascular blood system, but instead have an open circulatory system with a hemocoel that creates a blood-filled body cavity (Dow and Romero, 2010b). Additionally, the renal systems of insects are also aglomerular and the production of urine occurs through the malpighian tubules (the structural homolog of human kidneys) as opposed to kidney as seen in humans (Beyenbach and Liu, 1996).

Despite these gross anatomical differences, global transcriptome analysis between humans and *D. melanogaster* shows conserved homology (Chien et al., 2002). When mRNA analysis of important human and *D. melanogaster* transport proteins of the human renal system and *D. melanogaster* malpighian tubules were performed, close conservation was observed (Wang et al., 2004). Urate oxidase has been shown to be exclusively expressed in the malpighian tubules during the larval and adult stage where it produces uric acid for excretion (Wallrath et al., 1990). There have also been past studies that have proposed using or have used *D. melanogaster* malpighian tubules to model the human kidney and renal system (Beyenbach et al., 2010; Dow and Romero, 2010a). Previously, it had been shown that calcium oxalate kidney stones could be induced by ethylene glycol and the stones were large enough to be measured and quantified (Chen et al., 2011). Thus, given our current understanding, a *D. melanogaster* model of uric acid kidney stones formation induced by genetics and dietary purine manipulation represents a logical and powerful translational tool for modeling human uric acid kidney stones.

RNA interference (RNAi) utilizes endogenous short duplexed RNAs, either small interfering RNAs (siRNAs) or small hairpin RNAs (shRNAs), which are processed by an evolutionarily conserved mechanism for translational regulation. This conserved mechanism depends on enzymatic cleavage of siRNA or shRNA by the protein DICER (Ketting et al., 2001). The short processed RNA fragment is then incorporated into the RNA induced silencing complex (RISC) (Parrish et al., 2000). RISC, guided by the loaded short RNA fragment, then mediates the sequence specific silencing of target mRNAs through enzymatic cleavage (Bernstein et al., 2001; Fire et al., 1998; Hammond et al., 2000; Zamore et al., 2000).

A knockdown model in *Drosophila* can be created by breeding for flies possessing the desired transcription factor for an enhancer region upstream of a desired RNAi sequence. One

commonly used system based on this principle is the Gal4/UAS system initial found in *Saccharomyces cerevisiae* (Laughon et al., 1984) and subsequently adapted to *D. melanogaster* (Fischer et al., 1988). In the *D. melanogaster* Gal4/UAS system, gene expression is regulated by the binding of Gal4 transcription factors to *UAS* (*Upstream Activation Sequence*) enhancer sequences that control expression of downstream genes (Brand and Perrimon, 1993). Different patterns of Gal4 expressions are created by placing cell/tissue specific promoters upstream of the Gal4 transcription factor and this construct is termed a driver (Duffy, 2002). There are many drivers that have been developed to allow for reproducible spatiotemporal expression of genes downstream of *UAS* sequences. Driver strains are commercially available as well as *UAS* responder strain lines containing expressible RNAi sequences. A simple cross of a female fly containing driver X and male fly of responder line Y RNAi allows for controlled spatiotemporal expression of Y RNAi according to the promoter of X in the progeny. One variation of this system is called GeneSwitch (GS) Gal4 system. In the GeneSwitch Gal4 system, Gal4 transcription factor activity is induced by progesterone or progesterone analog hormone binding to Gal4 transcription factor (Ford et al., 2007; Han et al., 2000; Osterwalder et al., 2001; Roman et al., 2001), which allows for stricter temporal and spatial control of gene expression based on whether progesterone or a progesterone analog is administered as well as the rout of administration.

Using RNAi in conjunction with food supplementation to induce kidney stones in *D. melanogaster* has been accomplished in the past for calcium oxalate kidney stones (Hirata et al., 2012). In the study, the authors knocked down dPrestin, an anion transporter, and found that dPrestin influenced the excretion of calcium oxalate (Hirata et al., 2012). In another study, mineralization of calcium oxalate stones were induced by ethylene glycol, hydroxyl-l-proline,

and calcium oxalate (Chen et al., 2011). These mineralization of calcium oxalate stones were reduced by dietary supplementation of potassium citrate (Chen et al., 2011). There have also been numerous papers that have been written on the utility of the *D. melanogaster* for modeling kidney disorders and uric kidney stones disease (Dow and Romero, 2010a; Knauf and Preisig, 2011; Miller et al., 2013). Can this be accomplished for uric acid kidney stones? Performing that same procedure for uric acid kidney stones in *D. melanogaster* seems a logical step considering the previous success of applying RNAi and food supplementation for modeling calcium oxalate kidney stones and the success of modeling numerous other types of kidney disorders using the fly model (Chen et al., 2011; Dow and Romero, 2010a; Hirata et al., 2012; Knauf and Preisig, 2011; Miller et al., 2013).

Food supplementation is an ideal method of administering compounds when performing a screen for compounds to rescue a disease phenotype in *D. melanogaster*. Oral ingestion of food containing supplemented compounds mimics oral ingestion by humans, which is the most common method of consuming drugs. Oral ingestion of food supplemented with compounds also has the advantage of easy administration. To introduce a compound, the food supplemented with a compound can be easily exchanged in place of regular food. Many screens have already been successfully performed in *D. melanogaster* using food supplementation. For example, 88 chemotherapeutic compounds were tested for their effect on intestinal stem cells in *D. melanogaster* (Markstein et al., 2014). In another example, *D. melanogaster* was used in a screen of 2,000 compounds for their effect on a model of Fragile X Syndrome (Chang et al., 2008). A screen utilizing food supplementation with *D. melanogaster* is highly cost effective, requiring small amounts of compounds relative to larger model organisms like mice. Thus, food supplementation in *D. melanogaster* represents an efficient and effective way to deliver

compounds in a screen using our model. Taken together, *D. melanogaster* is exceptionally well suited for our proposed plan to induce uric acid kidney stone formation by knocking down urate oxidase using RNAi and supplementing purines to the diet.

As previously stated, functional urate oxidase is expressed in *D. melanogaster* while humans have a so-called pseudogene which is not expressed (Kratzer et al., 2014; Oda et al., 2002). Loss of urate oxidase expression and enzymatic activity have given way to massive elevation of uric acid in the serum from 0.4 to 0.7 mg/dl, as seen in many lower apes, to about 4 to 5 mg/dl currently observed in the average American (Johnson et al., 2005). This elevation of uric acid is problematic considering elevated uric acid can lead to gout and uric acid kidney stones. To compound the problem in addressing uric acid kidney stone disease, there currently are no viable or robust animal models of uric acid kidney stone disease.

Our overall goal is to address the lack of a disease model for human uric acid kidney stone disease. To accomplish this goal, we will develop a translational model of uric acid kidney stone disease in *D. melanogaster* by knocking down urate oxidase using RNAi in combination with dietary purine supplementation. We will then confirm the model forms uric acid kidney stones. Will urate oxidase knockdown in combination with dietary purine supplementation elevate uric acid levels and induce the formation of uric acid kidney stones in *D. melanogaster*? We hypothesize that if urate oxidase enzyme activity and dietary purine both play critical roles in uric acid kidney stone formation across species, then knocking down urate oxidase in combination with dietary purine supplementation will increase uric acid and uric acid kidney stone formation in *D. melanogaster*. We can measure uric acid levels using a colorimetric assay. We can then quantify the percentage of flies that formed uric acid kidney by dissecting the excretory system of *D. melanogaster* and visually checking for the presence or absence of uric

acid kidney stones in a binomial manner for each individual fly. We then calculated the average probability of forming uric acid kidney stone for each experimental condition.

If knocking down urate oxidase in combination with dietary purine supplementation is shown to increase uric acid kidney stone formation— can compounds currently used to treat gout and uric acid kidney stones in humans be used to reduce uric acid kidney stone formation when urate oxidase is knocked down in combination with dietary purine supplementation in our model? We hypothesize that if our model of uric acid kidney stones disease mimics human pathology, then supplementing compounds normally used to treat gout and uric acid kidney stones in humans, should reduce uric acid kidney stone formation when uric acid kidney stone formation is induced by urate oxidase knockdown and dietary purine supplementation. We can test this by supplementing allopurinol, a xanthine oxidase inhibitor used to treat gout and uric acid kidney stones in humans (Akkasilpa et al., 2004; Halabe and Sperling, 1994), and potassium citrate, a pH alkalizer used to treat uric acid kidney stones in humans (Maalouf, 2014; Sorkhi et al., 2011), when uric acid kidney stone formation is induced by urate oxidase knockdown in combination with dietary purine supplementation.

If compounds used to treat gout and uric acid kidney stones in humans are effective at reducing uric acid kidney stone formation in our model when urate oxidase is knocked down in combination with dietary purine supplementation— can compounds predicted to reduce gout and uric acid kidney stones in humans, but are not currently used for such purposes, reduce uric acid kidney stone formation when urate oxidase is knocked down in combination with dietary purine supplementation? We can perform this experiment by supplementing purine synthesis inhibitor methotrexate, diuretic hydrochlorothiazide, and pH alkalizer l-lysine to our model when uric acid

kidney stone formation is induced by urate oxidase knockdown in combination with dietary purine supplementation.

Lastly, we want find new compounds for the treatment of uric acid kidney stone disease using our model in a medium throughput screen. If we generate a model of uric acid kidney stone disease in *D. melanogaster* that forms uric acid kidney stones and the phenotype is successfully rescued using human treatments for gout and uric acid kidney stone as well as treatments predicted to be effective—can a medium throughput unbiased screen of compounds find candidate inhibitors of uric acid kidney stone disease. These candidate compounds can be further tested using the fly model or a yet to be developed murine model of uric acid kidney stone disease.

5 Aims

Aim 1:

The first aim of this research is to develop a translational model of uric acid kidney stone disease in *D. melanogaster*.

Rationale:

Because both gout and uric acid kidney stone disease are caused by excessive uric acid in the serum and urine respectively, we began to investigate ways to elevate uric acid and posed the question—would urate oxidase knockdown in combination with dietary purine supplementation induce uric acid kidney stone formation in an animal with functional urate oxidase such as *D. melanogaster*? If urate oxidase enzyme activity and dietary purine are both critical in the formation of uric acid kidney stones across species, then urate oxidase knockdown in combination with dietary purine supplementation should increase uric acid and uric acid kidney stone formation in *D. melanogaster*. In addition, previous experiments have shown that RNAi in conjunction with food supplementation can induce the formation of calcium oxalate kidney stones in *D. melanogaster* (Chen et al., 2011; Hirata et al., 2012), attesting to the applicability of this procedure for modeling uric acid kidney stone disease.

Hypothesis:

If urate oxidase enzyme activity and dietary purine are both critical in the formation of uric acid kidney stones across species, then urate oxidase knockdown in combination with dietary purine supplementation should increase uric acid and uric acid kidney stone formation in *D. melanogaster*.

Aim 2:

The second aim will be to test compounds currently used to treat gout and uric acid kidney stones in humans for their ability to reduce uric acid kidney stone formation in our model when uric acid kidney stone formation is induced by urate oxidase knockdown in combination with dietary purine supplementation. Compounds used to treat gout and uric acid kidney stones in humans should also be effective in our model if our model is translational and recapitulates human uric acid kidney disease.

Rationale:

If urate oxidase knockdown in combination with dietary purine supplementation is shown to induce uric acid kidney stone formation in *D. melanogaster*, the question arises whether compounds used to treat gout and uric acid kidney stones in humans can also reduce uric acid kidney stone formation in our model. We chose allopurinol and potassium citrate as two compounds to test. Allopurinol is used to treat human gout and uric acid kidney stones and works by lowering uric acid levels in the serum and urine through inhibition of xanthine oxidase, the enzyme that converts xanthine into uric acid (Akkasilpa et al., 2004; Eger et al., 2000; Halabe and Sperling, 1994; Sriranganathan et al., 2014). Potassium citrate is used to treat human uric acid kidney stones and works by alkalizing the urine pH and driving the formation of more soluble urate in urine (Maalouf, 2014; Sorkhi et al., 2011). Both these compounds work in treating human uric acid kidney stone disease and should work in our model if our model is translational and recapitulates human disease pathologies. This will initially help validate that our model conforms and responds as expected to treatments used in humans.

Hypothesis

If our model of uric acid kidney stone disease in *D. melanogaster* recapitulates human pathology and is translational, then supplementing allopurinol or potassium citrate in our model when urate oxidase is knocked down and dietary purine is supplemented should reduce the formation of uric acid kidney stones.

Aim 3:

The third aim of this research will be to test compounds not currently used to treat gout or uric acid kidney stone patients, but are predicted to be effective based on current literature.

Rationale:

Can we find new compounds to reduce gout and uric acid kidney stones using our model based on literature? We chose compounds that we predicted to be effective in treating uric acid kidney stones in humans based on literature, but which are not currently used for such purposes.

Since gout and uric acid kidney stones are both diseases of excessive level uric acid, an end product of purine metabolism, a logical question arises. Can a purine synthesis inhibitor reduce uric acid kidney stone formation in our model when urate oxidase is knocked down and dietary purine is supplemented to induce uric acid kidney stone formation? We chose to test, methotrexate (MTX), an inhibitor of *de novo* purine synthesis, which works by inhibiting dihydrofolate reductase during the essential conversion of dihydrofolate to active tetrahydrofolate for subsequent purine and pyrimidine nucleotide synthesis (Goodsell, 1999; Rajagopalan et al., 2002; Zhang et al., 2013). If purine synthesis contributes to uric acid kidney

stone formation when urate oxidase is knocked down and dietary purine is supplemented, purine synthesis inhibitors should reduce uric acid kidney stone formation in our model.

For the treatment of uric acid kidney stones in humans, it is recommended that patients stay hydrated to dilute and continuously flush their renal system of small stones (Choi et al., 2005). Can we supplement diuretics to reduce uric acid kidney stone formation in our model when urate oxidase is knocked down and dietary purine is supplemented to induce uric acid kidney stone formation? If diluting and continuously flushing the renal system can prevent uric acid kidney stone formation in humans, then supplementing diuretics should reduce the formation of uric acid kidney stones in our model when urate oxidase is knocked down and dietary purine is supplemented. We choose to test hydrochlorothiazide, a compound that has been shown to increase urine output in humans (Linton and O'Donnell, 1999) and has been shown to function in the same manner in the malpighian tubules of *D. melanogaster* (Linton and O'Donnell, 1999).

Lastly, we chose to test basic amino l-lysine (L-Lys) to see if we could reduce the formation of uric acid kidney stones by alkalizing the blood and urine pH. In humans, pH alkalization is an effective way to reduce uric acid kidney stones using potassium citrate (Maalouf, 2014; Sorkhi et al., 2011). Can, l-lysine, a basic amino acid, also reduce uric acid kidney stone formation in our model when urate oxidase is knocked down and dietary purine supplemented? If uric acid kidney stones formation can be reduced in humans by pH alkalizers, then supplementing l-lysine when urate oxidase is knocked down and dietary purine is supplemented should reduce uric acid kidney stone formation. Alkalizers effectively cause the formation of more soluble urate while reducing the levels of uric acid by increasing the pH above the pKa_1=5.7 of uric acid (Fig. 7).

Hypothesis:

If purine synthesis contributes to uric acid kidney stone formation when urate oxidase is knocked down and dietary purine supplemented, then supplementing a purine synthesis inhibitor like methotrexate should reduce uric acid kidney stone formation in our model.

If diluting and continuously flushing the renal system can prevent uric acid kidney stones in humans, then supplementing a diuretic like hydrochlorothiazide should reduce the formation of uric acid kidney stones in our model when urate oxidase is knocked down and dietary purine supplemented.

If uric acid kidney stone formation can be reduced by a pH alkalizer like potassium citrate in humans, then supplementing l-lysine, a basic amino acid, to our model when urate oxidase is knocked down and dietary purine is supplemented, should reduce uric acid kidney stone formation.

Aim 4:

The fourth aim of this research will be to use our validated *D. melanogaster* model of uric acid kidney stone disease to perform a medium throughput screen on 117 natural compounds for inhibitors of uric acid kidney stone formation.

Rationale:

After generating and validating our model by completing aim 1, aim 2, and aim 3, we will perform a medium throughput unbiased screen to find candidate compounds that can inhibit uric acid kidney stone formation. These candidate hits can be further tested to determine whether

their effect can be recapitulated in our fly model or another organism like mice. If our model recapitulates uric acid kidney stone disease as seen in humans and this model is validated by testing (aims 1-4), then a medium throughput screen for compounds to reduce uric acid kidney stone formation in an unbiased fashion should produce inhibitors of uric acid kidney stone formation. We chose a 117 natural compound library provided by the Nation Institute of Health for research testing to perform the medium throughput screen.

Hypothesis:

If our *D. melanogaster* model of uric acid kidney stone is authentic and compounds effective in treating human uric acid kidney stones are effective in reducing the formation of uric acid kidney stones, then a medium throughput 117 compound screen of natural compounds should provide us with a candidate inhibitor compounds that can reduce uric acid kidney stone formation.

6 Materials

6.1 *D. melanogaster* husbandry

Fly lines were maintained in 25 mm diameter x 95 mm length vials (Genesee, San Diego, CA, USA, 32-109RL) on stock food under standard conditions of 25 °C and 60% humidity on a 12 h light/dark cycle. When two lines were crossed, females from the driver line (who have hatched from their pupae less than 7 d prior) were placed into bottles (Genesee Scientific, #49-100) with males from the RNAi line (15 females:3 male) 14 d prior to 0 d (-14 d). Driver line females and RNAi line males were allowed to mate for 7 d and removed from the bottles at 7 d prior to 0 d (-7 d). Progeny were allowed to develop in the bottles for 7 d and female flies are sorted onto appropriate food conditions 7 d later (0 d).

6.2 Stock food for *D. melanogaster*

Stock food was composed of 1.5% SAF Instant Yeast (USA Emergency Supply, Colfax, North Carolina, USA, N016), 8.5% corn (Genesee Scientific, #62-101), 5% sugar (C&H Granulated Sugar, Crockett, CA, USA, 50 lbs), 0.46% agar (Genesee Scientific, #16-104) and 85% water by volume. 1% by volume mixture consisting of 41% proprionic acid (Fisher Scientific, Waltham, MA, USA, A242-212), 0.41% phosphoric acid (Sigma-Aldrich, St. Louis, MO, USA, P1386-1L), and 54.05% water was added to the food and mixed thoroughly. 75 ml of stock food was poured into 8 oz fly bottles (Genesee Scientific, #32-129F) and sealed with caps (Genesee Scientific, #49-100) and allowed to cool to room temperature.

6.3 Low-Purine (LP) and High Purine (HP) food

Low purine (LP) food was composed of 0.5% Bacto yeast extract (VWR, Radnor, PA, USA, #90000-722), 8.5% corn (Genesee Scientific, #62-101), 5% sugar (C&H Granulated Sugar), 0.46% agar (Genesee Scientific, #16-104) and 85% water by volume. High purine (HP) food was composed of 5% yeast extract, 8.5% corn, 5% sugar, 0.46% agar and 85% water by volume. The original yeast extract contains 4.9% purines by mass as calculated from information contained in the manufactures brochure (Table 1), and therefore LP food was 0.5% x 4.9% = 0.0245% by mass purines and HP food was 5% x 4.9% = 0.245% purines by mass purines, a 10 fold difference. For both types of food, the ingredients were mixed and brought to a boil. 1% by volume of a mixture consisting of 41% proprionic acid (Fisher Scientific, A242-212), 0.41% phosphoric acid (Sigma-Aldrich, P1386-1L), and 54.05% water was added to the food and mixed thoroughly. The 3-5 ml of the mixture was poured into fly vials (Genesee Scientific, #49-102) and cooled too room temperature.

6.4 GS food: LP (-/+) and HP (-/+)

GS food was made by adding a 0.34% by volume mixture of 58 mM mifepristone (Cayman Chemical, Ann Arbor, MI, USA, #10006317), a progesterone analog, dissolved in ethanol (95%). Mifepristone was added during the cooling period to make LP (+) or HP (+) food. Control LP (-) or HP (-) food contains 0.34% by volume of ethanol (95%) instead of mifepristone. The remainder of the cooking processes was identical to the procedure for making LP and HP food.

6.5 Compound supplemented Food:

LP, HP, LP (-/+) and HP (-/+) food can have additional compounds supplemented to the mixture. Compounds were dissolved in water along with other components of the food mixture. The remainder of the cooking processes was identical to the procedure for making LP and HP food.

6.6 HP (+) Diet Supplemented with Synthetic Purine Food

The HP (+) diet supplemented with synthetic purine food is composed of the HP (+) diet supplemented with 10 mM Adenine (Sigma Aldrich, A8626-25G) and 10 mM Guanine (Sigma Aldrich, G11950-100G).

7 Methods

7.1 Fly Lines

UO RNAi Line

The *Urate Oxidase RNAi* line contains homozygous RNAi constructs against urate oxidase mRNA on the 2nd chromosome downstream of the Gal4-*UAS*. The line was acquired from the Japanese National Institute of Genetics (JNIG, 2002). The RNAi sequence (7171R-1) is contained on the left arm of the 2nd chromosome between 7,775.4 KPB – 7,785.4 KPB (Fig. 10). The RNAi sequence binds to the target exon sequence of the urate oxidase (Uro-RA) mRNA at the 5'end, which causes enzymatic degradation of mRNA transcription and knock down of urate oxidase expression in our model (Fig. 10).

DaGS Driver Line

The *DaGS* driver line contains homozygous GS Gal4 transcription factors downstream of *Da* protein promoters. The GS Gal4 transcription factor is expressed in the same spatiotemporal pattern as Gal4 transcription factors in *Da* driver lines, but requires progesterone or a progesterone analog binding to activate *UAS* binding and promote expression of downstream sequences. Fly strain was acquired from the Benz Lab at Caltech Institute of Technology, Pasadena, CA.

7.2 qRT - PCR

7.2.1 RNA sample extraction

All steps were performed at room temperature unless otherwise stated using a Quick-RNA MiniPrep kit (Zymo Research, Irvine, CA, USA, #R1055). For each sample, 10 flies per condition were placed in a 1.5 ml Eppendorf tubes and 200 µl of RNA Lysis Buffer (Zymo Research, #R1055) was added and the mixture was homogenized using a pellet pestle (Kimble Chase Kontes, Vineland, New Jersey, USA, 749540-0000) and homogenizer (Kimble Chase Kontes, 749540-0000). An additional 400 µl of RNA Lysis Buffer (Zymo Research, #R1055) was added and the sample was centrifuged at 10,000 rpm for 1 min. 400 µl of supernatant was transferred to Spin-away Filter (Zymo Research, #R1055) in a collection tube and centrifuged at 10,000 rpm for 1 min. Flow through was collected, and 400 µl of ethanol (95%) was added and mixed with the sample. The entire sample mixture was transferred to a Zymo-Spin IIICG Column (Zymo Research, #R1055) and centrifuged at 10,000 rpm for 1 min and flow through

discarded. 400 µl of RNA Prep Buffer was added (Zymo Research, #R1055) and the samples were then centrifuged at 10,000 rpm for 30 s and flow through was discarded. 700 µl of RNA Wash Buffer (Zymo Research, #R1055) had ethanol added (according to the directions on the packaging) to each sample and centrifuged at 10,000 rpm for 30 s and flow through was discarded. Another 400 µl of RNA Wash Buffer (Zymo Research, #R1055) with ethanol was added and samples were centrifuged at 10,000 rpm for 2 min and flow through discarded. A Zymo-SpinIIICG Column (Zymo Research, #R1055) was placed in an RNAse-free 1.5 ml Eppendorf tube and 30 µl of DNAse/RNAse-free water was added. The sample was then centrifuged at 16,000 rpm for 30 s and flow through collected. The $OD_{260/280}$ was measured with a Nanodrop (Thermal Scientific, Waltham, MA, USA, 1000-UV/Vis) and diluted with RNAse free water to obtain a 1 µg / 1 µl of purified RNA.

7.2.2 RT-PCR

All preparation steps were performed on ice unless otherwise stated using a QuantiTect Kit (Qiagen, Venlo, Netherlands, 205313). 2 µl of 7x gDNA Wipeout Buffer (Qiagen, 205313) was added to 1 µl of 1 µg / 1 µl purified RNA plus 11 µl of DNAse / RNAse-free water in a PCR tube plate (Thermoscientific, Waltham, MA, USA, 3418) and incubated for 2 min at 42 °C in T100 Thermal Cycle (Biorad, Hercules, CA, USA, #186-1096) to eliminate genomic DNA. 6µl of a 1:4:1 mixture of Quantiscript RT (Qiagen, 205313), 5x Quantiscript RT Buffer (Qiagen, 205313), and RT primer mix of forward and reverse primers for urate oxidase and Tubulin 56D RA loading control. The mixture was incubated for, 15-30 min at 42°C, then 3 min at 95 °C using a T100 Thermal Cycle (Biorad, #186-1096), to obtain the final cDNA product of target transcripts (Fig. 9).

7.2.3 qRT-PCR

All steps were performed on ice unless otherwise stated using a SensiFast Sybr Kit (Bioline, London, UK, BIO-98020). Forward and reverse primers were diluted to 500 nM in RNAse-free water and No-ROX Sybr-Mix (Bioline, BIO-98020) were added to create a 5:2 master mix solution. 7 µl of the master mix was added to wells of a qRT-PCR plate (4titude, Surrey, UK, 4ti-0383) that contained 3 µl of diluted cDNA. The plate was sealed with accompanying foil (4titude, 4ti-0500). The plate was then spun shortly to 500 rpm and inserted into a LightCycler 480 (Roche, Panzberg, Upper Bavaria, Germany, 05015243001) and the fluorescence was measured. The sample was subjected to one denature cycle to 95 °C at 4.8 °C/s then a hold for 2 min. This was followed by 40 cycles between 60 °C (20 s hold) and 95 °C (5 s hold) for template amplification and qRT-PCR fluorescence measurement. The fluorescence measurement and calculation of amplification curve and C_t was analyzed with LightCycler 480 Software Version 1.5 provided by the manufacturer. ΔC_t values were then normalized to Tubulin 56D RA controls. $\Delta\Delta C_t$ values where calculated relative to experimental controls and given as a percentage from procedure underlined in a previous study (Schmittgen and Livak, 2008).

7.3 Colorimetric uric acid measurement

The Colorimetric uric acid measurement was performed using a BioVision Uric Acid Colorimetric Assay Kit (BioVision, Milpitas, CA, USA, K608-100). Uric Acid Probe was warmed to 37 °C for 2 min and mixed well. 200 µl of Uric Acid Assay Buffer was dissolved with Uric Acid Enzyme provided with the kit to make a Uric Acid Enzyme Mix. A master mix solution was made from Uric Acid Buffer, Uric Acid Probe, and Uric Acid Enzyme Mix in a

48:1:1 ratio. A sample of 5 flies per experimental condition was weighed and averaged to obtain an average mass per fly to normalize the final uric acid measurement. The flies were then homogenized in 1.5 ml Eppendorph tubes using a pellet pestle (Kimble Chase Kontes, 749520-0090) and homogenizer (Kimble Chase Kontes, 749540-0000) in 200 µl of Uric Acid Assay buffer for 45 s. The sample was then spun for 60 s at 10,000 rpm to form a pellet. 25 µl of supernatant was brought to 3 appropriate wells of a 96 well plate (Corning, Corning, NY, USA, #353916) for a total of 3 technical replicates per condition. 25 µl of Uric Acid Buffer was brought to each well. 50 µl of master mix was added per well and mixed gently to avoid air bubbles. At the same time, Uric Acid Standard Concentrations were created from Uric Acid Standard and Uric Acid Assay Buffer over 6 concentrations of uric acid (0.00 µg, 6.72 µg, 13.44 µg, 26.88 µg, 40.34 µg, and 53.79 µg). The 96-well plate was then covered in aluminum foil and incubated for 30 min at 37 °C. Colorimetric measurement was then performed using a fluorescence detection machine at OD_{570} (Molecular Devices, Sunnyvale, CA, USA, M2). Linear regression was performed in Excel (Microsoft, Redmond, WA, USA, Excel 2013) using the Uric Acid Standard Concentration measurements. $R^2 = 0.9983$. Uric acid concentration was then calculated from the linear equation of the best fit line. The uric acid concentration was then divided by the average weight of the original 5 flies per condition to normalize the final reading for differences in mass.

7.4 Micro-dissection of *D. melanogaster* excretory system

A fly was incapacitated using CO_2 gas and placed on a slide next to a droplet of water under a stereomicroscope (Zeiss, Jena, Germany, STEMI 2000-C). Under the stereomicroscope, forceps were used to hold down the thorax and grasp the anal plate. Slowly, the forceps were

used to separate the anal plate with gut and malpighian tubules attached from the fly abdominal cavity and into the droplet of water. The entire gut with malpighian tubules attached was completely excised from the fly and checked for uric acid stones concretions. This dissection protocol was adapted from a previous study (Tauc et al., 2014).

7.5 Uric acid kidney stone formation

Uric acid kidney stone formation was measured in a binomial manner for each individual fly and any stone(s) larger than 25 µm was counted as one and the absence of a stone or stones was counted as a zero for each respective fly. The % of stone formers was calculated as the number of flies that formed uric acid kidney stones divided by the total number per condition.

7.6 Medium throughput screen of 117 natural compounds

The HP (+) diet supplemented with synthetic purine food was cooked according to the corresponding protocol in the materials section and poured into 96-well plates (VWR, 15705-066) with 1 mm holes in the center of each well. The 96-well plates (VWR, 15705-066) were put on top of 1 ml 96-well masterblocks (VWR, 82051-244) and centrifuged at 4,000 rpm for 2 min and the food was allowed to cool for 3 h. 10 µl of each compound (200 µM) in dimethyl sulfoxide (1:50) (Alfa Aesar, Ward Hill, MA, USA, 43998) solution was administered on top of the HP (+) diet supplemented with synthetic purine food in each well of the 1 ml 96-well masterblocks (VWR, 82051-244) accordingly. The reference diet was the HP (+) diet supplemented with synthetic purine food topped with 10 µl of dimethyl sulfoxide (1:50) solution (Alfa Aesar, 43998) and the positive control was the HP (+) diet supplemented with synthetic

purine food topped with 10 µl of methotrexate (200 µM) (Sigma Aldrich, PHR1396-1G). The 1 ml 96-well masterblocks (VWR, 82051-244) were then centrifuged at 4,000 rpm for 2 min and the solutions delivered on top of the food are allowed to absorb into surface of the for 3 h. For the screen, there were 3 wells per condition and 5 flies per well were place into each well. The top of the 1 ml 96-well masterblocks (VWR, 82051-244) were covered with 96-well plates with 200 µm air holes and sealed with tape. Flies are housed at 29 °C and 60% humidity on a 12 h light/dark cycle. Every other day, flies are transferred from the old 1 ml 96-well masterblocks (VWR, 82051-244) into a new 1 ml 96-well masterblocks (VWR, 82051-244) with fresh compound solutions. Flies are dissected after 7 d.

The 117 compounds came from the natural compound products set III provided by the Developmental Therapeutics Program of the National Institute of Health (NTP, 2015).

7.7 Statistics

Student's two-tailed t-test analysis was performed as paired samples. *** = p-value < 0.001, ** = p-value < 0.01, * = p-value < 0.05. Confidence Intervals (CI) are calculated as 95%. Standard error of the mean is abbreviated SEM. All calculations were computed using Prism 4.03 Software (Muzyka et al., 1992-2005).

One-way analysis of variance (ANOVA) was performed as repeated measures and Tukey's multiple comparison tests were performed. *** = p – value < 0.0005, ** = p – value < 0.01, * = p – value < 0.05. Confidence intervals are calculated as 95%. All calculations were computed using Prism 4.03 software (Graphpad Software Inc, La Jolla, CA, USA).

8 Results

8.1 Efficient urate oxidase knockdown in *D. melanogaster* using RNAi

We first wanted to confirm that we had efficient knockdown of urate oxidase in our model using RNAi, therefore we performed qRT-PCR on urate oxidase mRNA in *Da > UO RNAi* (urate oxidase knockdown) flies and *Da > W1118* (control) flies fed the stock diet at 0 d. We observed that there was efficient knockdown of urate oxidase at 0 d and a significant decrease in urate oxidase mRNA transcripts over 11 biological replicates (Fig. 11A). At 0 d, urate oxidase mRNA in our urate oxidase knockdown flies was at 10% relative to control flies (Fig. 11A) and this knockdown was significant ($p < 0.001$). When we compared the ΔC_t value of urate oxidase knockdown flies relative to control flies, we observed that there was a significant reduction in urate oxidase mRNA (higher ΔC_t value) at 0 d over 11 biological replicates (Fig. 11B). To be specific, the ΔC_t value for urate oxidase knockdown flies substantially increased from 3.88 to 7.06 (Fig. 11B) and this increase was significant ($p < 0.001$).

Next, we wanted to see if urate oxidase knockdown remained efficient throughout adulthood and what effect dietary purine may have on urate oxidase expression, therefore we performed qRT-PCR on urate oxidase mRNA in *Da > UO RNAi* (urate oxidase knockdown) flies fed the LP and HP diets for 7 and 14 d (Fig. 11C). The LP food was 0.5% x 4.9% = 0.0245% by mass purines and the HP food was 5% x 4.9% = 0.245% purines by mass purines, which means the HP diet had 10 times more purines by mass than the LP diet. We observed knockdown of urate oxidase at 7 d on the LP diet but this knockdown was less efficient on the HP diet (Fig. 11C). This pattern was observed also at 14 d (Fig. 11C). At day 7, the relative

levels of urate oxidase mRNA in our urate oxidase knockdown flies were at 8% and 13% on the LP and HP diets compared to control flies respectively (Fig. 11C). At day 14, the relative levels of urate oxidase mRNA in our urate oxidase knockdown flies were at 15% and 36% on the LP and HP diets respectively compared to the control flies (Fig. 11C). Though only one biological replicate was performed, the consistent knockdown of urate oxidase over both the LP and HP diets at 7 and 14 d strongly suggests that our knockdown of urate oxidase was efficient and persisted throughout adulthood. Furthermore, urate oxidase expression appears to be upregulated when dietary purine was supplemented at both 7 and 14 d despite urate oxidase knockdown by RNAi.

8.2 Urate oxidase knockdown and dietary purine supplementation in *D. melanogaster* increased uric acid levels

After initially confirming that our urate oxidase knockdown was efficient, we then wanted to test if urate oxidase knockdown and dietary purine supplementation could increase uric acid levels. It is already known that reducing purine intake can effectively reduce uric acid and uric acid kidney stone formation in humans (Choi et al., 2005; Halabe and Sperling, 1994). To test if urate oxidase knockdown and dietary purine supplementation can increase uric acid levels in our model, we performed a colorimetric assay for uric acid in *DaGS > UO RNAi* (urate oxidase knockdown flies) fed the LP and HP diets with and without RNAi expression activator mifepristone (progesterone analog) after 7 and 14 d (Fig. 12). We observed that uric acid increased when urate oxidase was knocked down on the HP (+) diet compared to the LP (+) diet at 7 and 14 d (Fig. 12). On our control LP (-) and HP (-) diet, there was no activation of urate oxidase knockdown and dietary purine supplementation did not increase uric acid levels at 7 or

14 d compared to the LP (+) and HP (+) diets (Fig. 12). After 7 d, in control flies fed the LP (-) and HP (-) control diets compared to urate oxidase knockdown flies fed the LP (+) and HP (+) diets, uric acid was elevated and jumped from 50.3 µM to 54.7 µM ($p > 0.05$) and 67.3 µM to 68.33 µM respectively ($p > 0.05$) (Fig. 12). After 14 d, uric acid levels increased from 54.3 µM to 55.7 µM for the LP (-) diet compared to the LP (+) diet. For the HP (-) diet compared to HP (+) diet after 14 d, uric acid significantly increased from 88 µM to 155 µM ($p < 0.001$). In the control flies and urate oxidase knockdown flies, the HP diet tended to elevated uric acid levels regardless of whether urate oxidase was knocked down (Fig. 12). However, when urate oxidase was knocked down and dietary purine supplemented, elevation of uric acid was higher comparing the HP (-) and HP (+) diet at 14 d (Fig. 12). Strikingly, uric acid elevation appears to be time dependent and increases with age when we compare the uric acid levels at 7 d and 14 d (Fig. 12). Furthermore, urate oxidase knockdown further pushed uric acid levels higher relative to control flies (Fig. 12). These initial findings suggested that in our model, urate oxidase knockdown and dietary purine supplementation increased uric acid levels as we hypothesized. We further validated that urate oxidase knockdown and dietary purine supplementation increased uric acid levels by having collaborators perform LC/MS/MS to measure global levels of uric acid as well other important purine metabolites like adenine, adenosine, guanine, guanosine, and xanthine. When LC/MS/MS was performed, we saw that *DaGS > UO RNAi* (urate oxidase knockdown) flies fed the HP (+) diet had a four-fold increase in uric acid levels relative to uric oxidase knockdown flies fed the control HP (-) diet (data not shown). In parallel, allantoin decreased 1 order of magnitude also as expected while adenine, adenosine, guanine, and guanosine remained stable (data not shown).

8.3 Urate oxidase knockdown and dietary purine supplementation in *D. melanogaster* increased uric acid kidney stone formation

Next we wanted test if elevation of uric acid by urate oxidase knockdown and dietary purine supplementation can induced the formation of uric acid kidney stones. We performed micro-dissection and measured uric acid kidney stone formation in *DaGS > UO RNAi* (urate oxidase knockdown) flies fed the LP (+) and HP (+) diets and control flies fed the LP (-) and HP (-) control diets after 14 d in 3 separate biological trials (Fig. 13A). When dietary purines was supplemented and urate oxidase knocked down, the formation of uric acid kidney stones increased significantly for flies on the HP (+) diet compared to control flies fed the HP (-) control diet and uric acid kidney stone formation jumped from 8% to 72% ($p < 0.001$) (Fig. 13A). We took samples images of *DaGS > UO RNAi* (urate oxidase knockdown) flies fed the HP (+) diet and compared them to control flies fed the HP (-) control diet (Fig. 13C). From the pictures, the appearance of large concretions and mineralized structures can be observed visually (Fig. 13C). On the LP (-/+) diet, dietary purine supplementation in combination with urate oxidase knockdown did not induce uric acid kidney stone formation for either group, which remained at 0% (Fig. 13A). Next, we wanted to test if urate oxidase knockdown during development and during adulthood could also induce uric acid kidney stones when dietary purines were supplemented in adulthood using the *Da* driver. We performed micro-dissection and measured uric acid kidney stone formation in *Da > UO RNAi* (urate oxidase knockdown) flies and *Da > W1118* (control) flies fed the LP and HP diet after 14 d in 3 separate biological trials (Fig. 13B). When purines were supplemented in adulthood and urate oxidase knocked down during development and adulthood, the formation of uric acid kidney stones increased significantly for flies on the HP diet compared to control flies fed the LP diet, which jumped

from 0% to 50% ($p < 0.01$) (Fig. 13B). On the LP diet, urate oxidase knockdown did not increase uric acid kidney stone formation, which remained at 0% (Fig. 13B). Using two different drivers, we saw that regardless of when urate oxidase was knocked down, whether that was during adulthood or development and adulthood, urate oxidase knockdown and dietary purine supplementation induced uric acid kidney stones to form in our model of uric acid kidney stone disease.

8.4 Allopurinol and potassium citrate reduced uric acid kidney stone formation in our *D. melanogaster* model of uric acid kidney stone disease

After initially confirming that urate oxidase knockdown in combination with purine supplementation could elevate uric acid and induce the formation of uric acid kidney stones, we wanted to test if we could reduce uric acid kidney stone formation in our model using compounds currently utilized in the treatment of gout and uric acid kidney stone patients.

We first tested allopurinol, a compound used for the treatment of gout and uric acid kidney stones in humans (Akkasilpa et al., 2004; Halabe and Sperling, 1994). Allopurinol inhibits xanthine dehydrogenase, the enzyme that converts xanthine into uric acid, which reduces uric acid levels and uric acid kidney stone formation in humans (Elion et al., 1966; Halabe and Sperling, 1994; Sriranganathan et al., 2014). We performed micro-dissection and measured uric acid kidney stone formation in *Da > UO RNAi* (urate oxidase knockdown) flies fed the HP diet with and without allopurinol (10 mM) (Fig. 14A). We observed that allopurinol (10mM) significantly reduced uric acid kidney stone formation from 64% to 25% ($p < 0.05$) (Fig. 14A). To further confirm allopurinol was effective at reducing uric acid kidney stones, and could

reduce uric acid kidney stone formation even when urate oxidase was knocked downed during adulthood but not development, we then performed micro-dissection and measured uric acid kidney stone formation in *DaGS > UO RNAi* (urate oxidase knockdown) flies fed the HP (+) diet with and without allopurinol (10 mM) (Fig. 14B). Allopurinol significantly reduced uric acid kidney stone formation from 64% to 19% when we compared flies fed the HP (+) diet to the HP (+) diet supplemented with allopurinol ($p < 0.05$) (Fig. 14B).

We next tested potassium citrate, a pH alkalizer used to treat cystine kidney stones and uric acid kidney stones in humans (Sorkhi et al., 2011), to test if the compound was also effective at reducing uric acid kidney stone formation in our model. We performed micro-dissection and measured uric acid kidney stone formation in *DaGS > UO RNAi* (urate oxidase knockdown) flies fed the HP (+) diet with and without potassium citrate (200mM) (Fig. 14C). We observed a significant reduction of uric acid kidney stone formation from 56% to 3% when we compared flies fed the HP (+) diet to flies fed the HP (+) diet supplemented with potassium citrate ($p < 0.001$) (Fig. 14C). To test whether potassium citrate can reduce uric acid kidney stone formation in a dose dependent manner, we me supplemented 10, 50, 100, and 200 mM of potassium citrate to the HP (+) diet and measured uric acid kidney stone formation (Fig. 14D). We observed that potassium citrate reduced uric acid kidney stone formation to 35%, 21%, 14%, and 0.0% when 10, 50, 100, and 200 mM of potassium citrate was supplemented to the diet HP (+) diet respectively (Fig. 14D). The trend showed a dose dependent reduction in uric acid kidney stone formation when potassium citrate was supplemented (Fig. 14D). Potassium citrate reduced uric acid kidney stone formation to almost 0% when 200 mM was supplemented over three experimental trials (n=3) (Fig. 14C) and an additional trial in a single separate experiment (n=1)

(Fig 14D), which argues for the effectiveness of potassium citrate as in treating uric acid kidney stones in our model.

8.5 Compounds predicted to be effective against uric acid kidney stones formation; methotrexate, hydrochlorothiazide, and l-lysine reduced uric acid kidney stone formation in our model

We saw that compounds used to treat gout and uric acid kidney stones in humans were effective at reducing uric acid kidney stone formation when urate oxidase was knocked down and dietary purine supplemented in our model. Next we wanted to test if compounds predicted to reduce uric acid kidney stone formation from the literature, could reduce uric acid kidney stone formation in our model when urate oxidase was knocked down and dietary purine supplemented. We chose methotrexate, a *de novo* purine synthesis inhibitor (Goodsell, 1999; Rajagopalan et al., 2002). We performed micro-dissection and measured uric acid kidney stone formation in *DaGS > UO RNAi* (urate oxidase knockdown) flies fed the HP (+) diet without and with methotrexate (5, 50, and 500 µM) supplemented (Fig. 15A). Supplementing 5, 50, and 500 µM of methotrexate to our urate oxidase knockdown flies supplemented dietary purines, significantly reduced uric acid kidney stone formation from 64% to 17%, 6%, and 0% respectively (Fig. 15A). At the highest concentration of 500 µM, methotrexate significantly reduced uric acid kidney stone formation to 0% ($p < 0.001$) (Fig. 15A).

L-lysine was also effective at reducing uric acid kidney stone formation (Fig. 15A). When micro-dissection was performed and uric acid kidney stone formation measured in *DaGS > UO RNAi* (urate oxidase knockdown) flies, uric acid kidney stone formation was moderately

reduced from 64% to 44%, 30%, and 17% when 10 µM, 100 µM, and 1000 µM of l-lysine was supplemented to the HP (+) diet respectively (Fig. 15A). At the highest concentration of 1000 µM, l-lysine significantly reduced uric acid kidney stone formation to 17% ($p < 0.001$) (Fig. 15A). Similarly, hydrochlorothiazide was also effective at reducing uric acid kidney stone formation from 64% to 47%, 39%, and 31% when 10, 100, and 1000 µM of hydrochlorothiazide were supplemented to the HP (+) diet respectively (Fig. 15A). At the highest concentration of 1000 µM, hydrochlorothiazide significantly reduced uric acid kidney stone formation to 31% ($p < 0.001$) (Fig. 15A).

Of the three compounds tested, the most effective at reducing uric acid kidney stone formation was methotrexate (Fig. 15A). We wanted to further test our strongest candidate compound, methotrexate, therefore we then performed micro-dissection and measured uric acid kidney stone formation in *Da > UO RNAi* (urate oxidase knockdown) flies fed the LP diet and the HP diet with and without methotrexate over three different concentrations (5, 50, 500 µM) and in *Da > W1118* (control) flies fed the LP and HP diet after 14 d (Fig. 15B). We observed that increasing methotrexate concentration reduced uric acid kidney stone formation in a dosage dependent manner over 3 biological replicates (Fig. 15B). When 5, 50, and 500 µM of methotrexate was supplemented to the HP (+) diet, uric acid kidney stone formation was significantly reduced from 50% to 14%, 0%, and 0% respectively (Fig. 15B). At the highest concentration of 500 µM, methotrexate significantly reduced uric acid kidney stone formation to 0% ($p < 0.001$) (Fig. 15B). When both experiments are taken together, methotrexate appears to be an effective and robust compound for reducing uric acid kidney stone formation in our model.

8.6 Medium throughput compound screen of 117 natural compounds finds 7 inhibitors and 6 enhancers of uric acid kidney stone formation in our *D. melanogaster* model of uric acid kidney stone disease

We then performed a medium throughput natural compound screen using compounds from the Natural Products set III from the Nation Therapeutics Program of the National Institute of Health. We administered the compounds to *DaGS > UO RNAi* (urate oxidase knockdown) flies fed a HP (+) diet supplemented synthetic purines adenine (10 mM) and guanine (10 mM). We found Uric Acid Kidney Stone Inhibitors (UAKSIs) 1, 2, 3, 4, 5, 6, and 7 and Uric Acid Kidney Stone Enhancers (UAKSEs) 1, 2, 3, 4, 5, and 6. We categorized inhibitors that reduced the formation of uric acid kidney stone formation to less than 20% and enhancers that increased uric acid kidney stone formation to 80% or more. Our urate oxidase knockdown flies fed the reference HP (+) diet supplemented with synthetic purines and topped with dimethyl sulfoxide had 72% uric acid kidney stone formation (Fig. 18). Our positive control, knockdown flies fed the HP (+) diet with synthetic purines topped with methotrexate (200 μM), had 8% uric acid kidney stone formation (Fig. 18). Methotrexate decreased uric acid kidney stone formation and this was consistent with previous experiments that showed a robust decrease in uric acid kidney stone formation when methotrexate was supplemented to urate oxidase knockdown flies fed the HP diet (Fig. 14-15).

9 Discussion

The total number of people who suffer from accumulation of uric acid deposits or elevated uric acid levels is enormous. In the US alone, from 2007-2008, there were a total of 8.3 million patients who suffered from gout (Zhu et al., 2011). The total cost of treating patients with gout was estimated to be around 7.7 billion dollars for; inpatient and outpatient care, prescription drugs, emergency room visits, and other costs (Cisternas et al., 2009). The number of patients who will suffer from uric acid kidney stones at least once in their life in the US is estimated to be between 1.5 and 4.2 million patients (Bushinsky, 2001; Stamatelou et al., 2003). The probability of uric acid kidney stones reoccurrence after the first episode increases 23% and each subsequent episode further increases that probability (Trinchieri et al., 1999b). A very conservative estimate of the total cost of treating patients who suffer from uric acid kidney stones in the US, is around 300 million dollars annually (Bushinsky, 2001; Campion et al., 1987; Lotan, 2009; Walker et al., 2013). Taken together, the total number of people affected by accumulation of uric acid deposits or uric acid kidney stones disease is a staggering 9.8 million and the total cost is an enormous sum of 8 billion dollars. Finding new and innovative solutions for these patients that are effect remains a major challenge in urology and healthcare in general.

To compound the problem, there are no viable models of uric acid kidney stone disease in mice, no model exists in *D. melanogaster* all together, and uric acid kidney stone has yet to be modeled in any other model organism, highlighting the need for the development of such a model. There is a murine urate oxidase knockout model, but the murine model shows high lethality with 65% of the homozygous mutant mice dying within 4 weeks of birth unless maintained on allopurinol to reduce the extremely high levels or uric acid in the serum and urine (Wu et al., 1994). Other types of kidney stones, like cystinuria, have a viable murine model that

can recapitulate the disease phenotype. For example, a SLC7A9 knockout mouse model was created that is viable and forms cystinuria kidney stones and this disease phenotype can be rescued by administration of d-penicillin or mercaptopropionylglycine, also known as tiopronin (Font-Llitjos et al., 2007). In *D. melanogaster,* there have been previous work that have successfully modeled calcium oxalate kidney stones and other kidney stone associated disorders by using RNAi and food supplementation that showed the possibility of modeling uric acid kidney stone disease in a similar way (Chen et al., 2011; Hirata et al., 2012; Knauf and Preisig, 2011; Miller et al., 2013). To address the lack of a disease model for uric acid kidney stones, we successfully created a model of uric acid kidney stone disease in *D. melanogaster* by using RNAi and dietary modulation.

9.1 Validation of *D. melanogaster* model of uric acid kidney stone disease

We validated our model using; qRT-PCR to measure mRNA levels of urate oxidase, a colorimetric assay to measure uric acid levels, and performed micro-dissection to measure uric acid kidney stone formation (Fig. 11-13). We first confirmed the efficient knockdown of urate oxidase in our model using qRT-PCT (Fig. 11). After confirming our knockdown was efficient, we supplemented our urate oxidase knockdown flies with a high purine diet to induce uric acid kidney stone formation (Fig. 11-13). If urate oxidase enzyme activity and dietary purine are both critical in the formation of uric acid kidney stones across species, then urate oxidase knockdown in combination with dietary purine supplementation should increase uric acid and uric acid kidney stone formation in *D. melanogaster*. We saw that our model could be induced to form uric acid kidney stones when urate oxidase was knocked down and purine supplemented to the diet (Fig. 11-13). Uric acid levels increased with urate oxidase knockdown and dietary purine

supplementation and also appeared to increase with age (Fig. 12). Lastly and most importantly, we visually confirmed, then measured uric acid kidney stone formation and saw that it increased when uric acid was knocked down and purines supplemented (Fig. 13C). These findings further reaffirm the role of dietary purine in modulating uric acid levels that was previously seen in humans (Choi et al., 2005; Halabe and Sperling, 1994; Hediger et al., 2005; Johnson et al., 2005).

9.2 Testing human gout and uric acid kidney stone treatments using *D. melanogaster* model of uric acid kidney stone disease

After initially confirming that urate oxidase knockdown was efficient and dietary purine supplementation could induce uric acid kidney stone formation (Fig. 11-13). We tested whether compounds currently used to treat gout and uric acid kidney stones in humans, like allopurinol and potassium citrate, were also effective at treating uric acid kidney stones in our model (Fig. 14A-C). If our model of uric acid kidney stone disease in *D. melanogaster* recapitulates human pathology and is translational, then supplementing allopurinol or potassium citrate in our model when urate oxidase was knocked down and dietary purine supplemented should reduced the formation of uric acid kidney stones. We saw that, both allopurinol and potassium citrate were effective at reducing uric acid kidney stone formation (Fig.14A-D). Allopurinol inhibits xanthine dehydrogenase, the enzyme that converts xanthine into uric acid (Fig. 16) (Eger et al., 2000), and is used to treat gout and uric acid kidney stones in humans (Akkasilpa et al., 2004; Halabe and Sperling, 1994). Therefore, supplementing allopurinol should decrease uric acid levels and inhibit uric acid kidney stone formation by preventing the conversion of xanthine into uric acid

(Fig. 16). We observed the predicted reduction in uric acid kidney stone formation when allopurinol was tested (Fig. 14A-B). When pH alkalizer potassium citrate was tested, the compound also reduced uric acid kidney stone formation (Fig. 14C-D). Potassium citrate increases the pH, which drives the formation of more soluble urate and thus reduces uric acid and uric acid kidney stone formation (Fig. 16). Uric acid kidney stone formation was reduced when allopurinol or potassium was supplemented to our uric acid kidney stone model (Fig. 14A-C), which further substantiates our model as being translation and applicable for modeling human uric acid kidney stone disease. Given the two compounds are from distinct chemical classes, and yet are able to reduce uric acid kidney stone formation in humans and in our model as predicted, it is likely that major core components of human uric acid kidney stone disease are recapitulated in our *D. melanogaster* model of uric acid kidney stone disease.

9.3 Testing of compounds predicted to reduce uric acid kidney stone formation using *D. melanogaster* model of uric acid kidney stone disease

In the realm of pharmacology, one compound or drug can have multiple off target effects and the phenomenon is called polypharmacology (Apsel et al., 2008; Hopkins, 2008; Simon et al., 2011). One of the most famous example is Viagra, a phosphodiesterase inhibitor that was originally developed to treat ischemic heart disease and hypertension, is now most frequently used to treat erectile dysfunction (DeBusk et al., 2004). Another example is Aspirin; an analgesic used to relieve minor aches and pains is also used as a non-steroidal anti-inflammatory drug for rheumatoid arthritis (Simpson et al., 1966), Kawasaki disease (Durongpisitkul et al., 1995), and pericarditis (Berman et al., 1981) to name a few.

With this in mind, we tested known compounds, which are not currently used in the treatment of gout or uric acid kidney stone disease in humans, like methotrexate, hydrochlorothiazide, and l-lysine, but are predicted from literature to reduce uric acid kidney stone formation (Fig. 15A). We observed that methotrexate was most effective at reducing uric acid kidney stone formation in our model when urate oxidase was knocked down and dietary purine supplemented (Fig. 15A-B). Methotrexate effectively reduced uric acid kidney stone formation in a robust manner across different concentrations using two different drivers (Fig. 15A-B). Methotrexate inhibits dihydrofolate reductase in the essential conversion of dihydrofolate into tetrahydrofolate for purine synthesis and thus should reduce purine load and uric acid kidney stone formation by reducing the flow of purines through the entire purine pathway (Fig. 16). Furthermore, methotrexate reduced uric acid kidney stone formation to 0% at higher concentrations of 50 and 500 µM using both *Da* and *DaGS* drivers (Fig. 15A-B). Hydrochlorothiazide and l-lysine were also effective at reducing uric acid kidney stone formation in our model when urate oxidase was knocked down and dietary purine supplemented, but was less potent when compared to methotrexate (Fig. 15A-B). At higher concentrations of 100 and 1000 µM, hydrochlorothiazide and l-lysine could not robustly reduce uric acid kidney stone formation to 0% as methotrexate could at lower concentrations of 5 and 50 µM (Fig. 15A-B). Given those results, methotrexate appears to be extremely effective at reducing uric acid kidney stone formation in our model, and had greater potency compared to other tested compounds like l-lysine and hydrochlorothiazide.

Hydrochlorothiazide, a diuretic, was shown to reduce uric acid kidney stone in a dose dependent manner (Fig. 15A). In humans, hydrochlorothiazide works by inhibiting reabsorption of Na^+ from the lumen of distal convoluted tubule by NA^+Cl^- co-transporter into apical membrane

cells, which reduces the passive reabsorption of water that follows the non-reabsorbed sodium into the urine (Fig. 17) (Ali et al., 2012; Ecelbarger and Tiwari, 2006). It has also been shown that administering mineral water to patients that formed calcium oxalate kidney stones to increase urine output, decreased the overall occurrence of calcium oxalate kidney stones (Trinchieri et al., 1999a). One possible explanation may be that increasing urine output also eliminates small stones and concretions before growth to a size sufficient to block the urinary tract (Fig. 17). In *D. melanogaster*, basolateral Na^+Cl^- co-transporters of the malpighian tubules have been shown to play a significant role in ion exchange (Linton and O'Donnell, 1999). It is therefore possible that hydrochlorothiazide reduced uric acid kidney stone formation in our experiment in a similar manner by increasing urine flow (Fig. 17). A future experiment to validate this hypothesis could be to knockdown urate oxidase to induce uric acid kidney stone formation and overexpress of Na^+Cl^- co-transporters in parallel. Overexpression of Na^+Cl^- co-transporters should reduce uric acid kidney stone formation. Other hormones that drive water secretion in flies like Cap2b, kinin, or DH44 can also be used to further test and validate whether increased urine output can reduce uric acid kidney stones in our model.

L-lysine, a basic amino acid, was also shown to reduce uric acid kidney stone formation in a dosage dependent manner (Fig. 15A). Currently, urine alkalization is the main treatment option of choice to reduce uric acid kidney stones formation (Dardamanis, 2013). Given these facts, one possible explanation for these findings is that l-lysine alkalizes the urine. Higher pH levels above the pKa_1 of uric acid (pKa=5.7) (McCrudden, 2008), causes the formation of more soluble urate from less soluble uric acid (Fig. 7) (Fig. 16), which decreases the overall level of uric acid (Fig.16). One possible future experiment to test whether l-lysine is reducing uric acid kidney stone formation through alkalization would be to feed urate oxidase knockdown flies l-

lysine and collect the urine to test the pH. Another possible explanation may be that l-lysine, which is positively charged, surrounds and neutralizes the negatively charged uric acid stones. We could test this hypothesis by feeding urate oxidase knockdown flies isotope labeled l-lysine and tracing where the labeled l-lysine accumulates. If l-lysine chelates uric acid kidney stones and prevents further growth, then isotope labeled l-lysine should accumulate around uric acid kidney stones in our fly model when uric acid kidney stones formation is induced.

Our most effective compound methotrexate, a compound used for treatment of cancer and auto immune disease in humans (Goodsell, 1999; Rajagopalan et al., 2002; Wright et al., 1964), reduced uric acid kidney stone formation to 0% at 50 and 500 μM utilizing both the *Da* and *DaGS* driver (Fig. 15A-B). Methotrexate inhibits purine synthesis by competitively binding dihydrofolate reductase during the essential conversion of dihydrofolate to active tetrahydrofolate in the nucleotide synthesis pathway (Fig. 16) (Goodsell, 1999; Rajagopalan et al., 2002). In contrast, overexpression or hyper activity of the enzyme PRPP synthetase, which catalyzes the first step of purine synthesis, has the opposite effect of inducing elevated uric acid levels in the serum (Becker et al., 1986; Fujimori, 1996; Tatibana, 1996; Yamada et al., 2014; Yamada et al., 2010). These results reaffirm the validity of our model given that inhibition of *de novo* purine synthesis is expected to alleviate hyperuricemia and uric acid kidney stones by reducing the overall flow of purine through metabolism, salvage, degradation, and excretion (Fig. 16). An interesting experiment would be to measure metabolomic data on major purine nucleotides and purine metabolites in flies that are induced to form uric acid kidney stones by urate oxidase knockdown and dietary purine supplementation compared to those same flies supplemented methotrexate. If the overall flow of purine metabolites through purine metabolism, salvage, degradation, and excretion decreases, then this trend should be discernible from

metabolomic data. Even though methotrexate appears to be an extremely effective compound for treating uric acid kidney stone disease, the immune suppressant effects of methotrexate are problematic when treating human patients. Patients who are fighting infections or may encounter infections are at risk of fatal complications. An alternative compound or compounds that can reduce uric acid kidney stone formation but does not suppress the immune system is preferable. However, the model we created will allow us the opportunity to screen for compounds that can effectively treat uric acid kidney stones but have fewer deleterious effects.

9.4 Medium throughput screen of 117 compounds using *D. melanogaster* model of uric acid kidney stone disease finds seven inhibitors and six enhancers.

When we used our *D. melanogaster* model of uric acid kidney stone disease to screen 117 compounds from the Natural Compound Products Set III provided by the Developmental Therapeutics Program of the National Institute of Health ((NTP, 2015). We found 7 inhibitors; UAKSI1, UAKSI2, UAKSI3, UAKSI4, UAKSI5, UAKSI6, and UAKSI7 when we performed the medium throughput screen (Fig. 18). We also found 6 enhancers; UAKSE1, UAKSE2, UAKSE3, UAKSE4, UAKSE5, and UAKSE6 when we performed the medium throughput screen (Fig. 18). No discernible pattern appears from the list of inhibitors and enhancers that were found during the medium throughput screen (Fig. 18). Anti-tumorgenic compounds appear to be randomly distributed as inhibitors and enhancers of uric acid kidney stone formation. Further testing of individual compounds is required to further understand the mechanism by which uric acid kidney stone formation is reduced in our model for each respective compound.

9.5 Future experimental plans

In the future, we plan to transfer the results from our *D. melanogaster* model of uric acid kidney stone disease to a murine model. The murine model we will pursue would give us another tool to study uric acid kidney stone disease. Using oxonic acid, an inhibitor of urate oxidase in mice, we plan to elevate uric acid and recapitulate uric acid kidney stone disease in mice much like in our fly model. We will then test drugs and compounds for their ability to reduce uric acid kidney stones using this murine model. First, we will likely test methotrexate and the data and results should verify and validate findings found in our fly model. We also plan to execute a larger compound screen with thousands of compounds from the National Institute of Health using our fly model. By fully developing both a fly and murine model of uric acid kidney stone disease, we hope to be able to find novel solutions to treat patients who suffer from an accumulation of uric acid deposits or elevated uric acid levels, which number 9.8 million in the U.S. alone (Bushinsky, 2001; Stamatelou et al., 2003; Walker et al., 2013).

10 References

Akkasilpa, S., Osiri, M., Deesomchok, U., and Avihingsanon, Y. (2004). The efficacy of combined low dose of Allopurinol and benzbromarone compared to standard dose of Allopurinol in hyperuricemia. J Med Assoc Thai *87*, 1087-1091.

Ali, S.S., Sharma, P.K., Garg, V.K., Singh, A.K., and Mondal, S.C. (2012). The target-specific transporter and current status of diuretics as antihypertensive. Fundam Clin Pharmacol *26*, 175-179.

Altschul, S.F., Madden, T.L., Schaffer, A.A., Zhang, J., Zhang, Z., Miller, W., and Lipman, D.J. (1997). Gapped BLAST and PSI-BLAST: a new generation of protein database search programs. Nucleic Acids Res *25*, 3389-3402.

Apsel, B., Blair, J.A., Gonzalez, B., Nazif, T.M., Feldman, M.E., Aizenstein, B., Hoffman, R., Williams, R.L., Shokat, K.M., and Knight, Z.A. (2008). Targeted polypharmacology: discovery of dual inhibitors of tyrosine and phosphoinositide kinases. Nature chemical biology *4*, 691-699.

Bauer, M., Katzenberger, J.D., Hamm, A.C., Bonaus, M., Zinke, I., Jaekel, J., and Pankratz, M.J. (2006). Purine and folate metabolism as a potential target of sex-specific nutrient allocation in Drosophila and its implication for lifespan-reproduction tradeoff. Physiol Genomics *25*, 393-404.

BD-Bioscience (2006). BD Bionutrients™ Technical Manual Advanced Bioprocessing (3rd ed rev).

Becker, M.A., Losman, M.J., Rosenberg, A.L., Mehlman, I., Levinson, D.J., and Holmes, E.W. (1986). Phosphoribosylpyrophosphate synthetase superactivity. A study of five patients with catalytic defects in the enzyme. Arthritis Rheum *29*, 880-888.

Belenky, P., Bogan, K.L., and Brenner, C. (2007). NAD+ metabolism in health and disease. Trends Biochem Sci *32*, 12-19.

Berman, J., Haffajee, C.I., and Alpert, J.S. (1981). Therapy of symptomatic pericarditis after myocardial infarction: retrospective and prospective studies of aspirin, indomethacin, prednisone, and spontaneous resolution. American heart journal *101*, 750-753.

Bernstein, E., Caudy, A.A., Hammond, S.M., and Hannon, G.J. (2001). Role for a bidentate ribonuclease in the initiation step of RNA interference. Nature *409*, 363-366.

Beyenbach, K.W., and Liu, P.L. (1996). Mechanism of fluid secretion common to aglomerular and glomerular kidneys. Kidney Int *49*, 1543-1548.

Beyenbach, K.W., Skaer, H., and Dow, J.A. (2010). The developmental, molecular, and transport biology of Malpighian tubules. Annu Rev Entomol *55*, 351-374.

Boss, G.R., and Seegmiller, J.E. (1982). Genetic defects in human purine and pyrimidine metabolism. Annu Rev Genet *16*, 297-328.

Brand, A.H., and Perrimon, N. (1993). Targeted gene expression as a means of altering cell fates and generating dominant phenotypes. Development *118*, 401-415.

Bushinsky, D.A. (2001). Kidney stones. Adv Intern Med *47*, 219-238.

Campion, E.W., Glynn, R.J., and DeLabry, L.O. (1987). Asymptomatic hyperuricemia. Risks and consequences in the Normative Aging Study. Am J Med *82*, 421-426.

Chang, S., Bray, S.M., Li, Z., Zarnescu, D.C., He, C., Jin, P., and Warren, S.T. (2008). Identification of small molecules rescuing fragile X syndrome phenotypes in Drosophila. Nat Chem Biol *4*, 256-263.

Chen, Y.-H., Liu, H.-P., Chen, H.-Y., Tsai, F.-J., Chang, C.-H., Lee, Y.-J., Lin, W.-Y., and Chen, W.-C. (2011). Ethylene glycol induces calcium oxalate crystal deposition in Malpighian tubules: a Drosophila model for nephrolithiasis/urolithiasis. Kidney international *80*, 369-377.

Chien, S., Reiter, L.T., Bier, E., and Gribskov, M. (2002). Homophila: human disease gene cognates in Drosophila. Nucleic Acids Res *30*, 149-151.

Choi, H.K., Liu, S., and Curhan, G. (2005). Intake of purine-rich foods, protein, and dairy products and relationship to serum levels of uric acid: the Third National Health and Nutrition Examination Survey. Arthritis Rheum *52*, 283-289.

Cisternas, M.G., Murphy, L.B., Yelin, E.H., Foreman, A.J., Pasta, D.J., and Helmick, C.G. (2009). Trends in medical care expenditures of US adults with arthritis and other rheumatic conditions 1997 to 2005. J Rheumatol *36*, 2531-2538.

Dardamanis, M. (2013). Pathomechanisms of nephrolithiasis. Hippokratia *17*, 100-107.

DeBusk, R.F., Pepine, C.J., Glasser, D.B., Shpilsky, A., DeRiesthal, H., and Sweeney, M. (2004). Efficacy and safety of sildenafil citrate in men with erectile dysfunction and stable coronary artery disease. The American journal of cardiology *93*, 147-153.

Dow, J.A., and Romero, M.F. (2010a). Drosophila provides rapid modeling of renal development, function, and disease. American Journal of Physiology-Renal Physiology *299*, F1237-F1244.

Dow, J.A., and Romero, M.F. (2010b). Drosophila provides rapid modeling of renal development, function, and disease. American Journal of Physiology Renal Physiol *299*, 1237-1244.

Duffy, J.B. (2002). GAL4 system in Drosophila: a fly geneticist's Swiss army knife. Genesis *34*, 1-15.

Durongpisitkul, K., Gururaj, V.J., Park, J.M., and Martin, C.F. (1995). The prevention of coronary artery aneurysm in Kawasaki disease: a meta-analysis on the efficacy of aspirin and immunoglobulin treatment. Pediatrics *96*, 1057-1061.

Ecelbarger, C.A., and Tiwari, S. (2006). Sodium transporters in the distal nephron and disease implications. Curr Hypertens Rep *8*, 158-165.

Edelstein, L. (1943). The Hippocratic Oath: Text, Translation and Interpretation (Baltimore: Johns Hopkins University Press).

Eger, B.T., Okamoto, K., Enroth, C., Sato, M., Nishino, T., Pai, E.F., and Nishino, T. (2000). Purification, crystallization and preliminary X-ray diffraction studies of xanthine dehydrogenase and xanthine oxidase isolated from bovine milk. Acta Crystallogr D Biol Crystallogr *56*, 1656-1658.

Elion, G.B., Kovensky, A., Hitchings, G.H., Metz, E., and Rundles, R.W. (1966). Metabolic studies of allopurinol, an inhibitor of xanthine oxidase. Biochemical pharmacology *15*, 863-880.

Enomoto, A., Kimura, H., Chairoungdua, A., Shigeta, Y., Jutabha, P., Cha, S.H., Hosoyamada, M., Takeda, M., Sekine, T., Igarashi, T.*, et al.* (2002). Molecular identification of a renal urate anion exchanger that regulates blood urate levels. Nature *417*, 447-452.

Enroth, C., Eger, B.T., Okamoto, K., Nishino, T., Nishino, T., and Pai, E.F. (2000). Crystal structures of bovine milk xanthine dehydrogenase and xanthine oxidase: structure-based mechanism of conversion. Proc Natl Acad Sci U S A *97*, 10723-10728.

Fire, A., Xu, S., Montgomery, M.K., Kostas, S.A., Driver, S.E., and Mello, C.C. (1998). Potent and specific genetic interference by double-stranded RNA in Caenorhabditis elegans. Nature *391*, 806-811.

Fischer, J.A., Giniger, E., Maniatis, T., and Ptashne, M. (1988). GAL4 activates transcription in Drosophila. Nature *332*, 853-856.

Font-Llitjos, M., Feliubadalo, L., Espino, M., Cleries, R., Manas, S., Frey, I.M., Puertas, S., Colell, G., Palomo, S., Aranda, J.*, et al.* (2007). Slc7a9 knockout mouse is a good cystinuria model for antilithiasic pharmacological studies. Am J Physiol Renal Physiol *293*, F732-740.

Ford, D., Hoe, N., Landis, G.N., Tozer, K., Luu, A., Bhole, D., Badrinath, A., and Tower, J. (2007). Alteration of Drosophila life span using conditional, tissue-specific expression of transgenes triggered by doxycyline or RU486/Mifepristone. Exp Gerontol *42*, 483-497.

Frassetto, L., and Kohlstadt, I. (2011). Treatment and prevention of kidney stones: an update. American family physician *84*, 1234.

Fujimori, S. (1996). [PRPP synthetase superactivity]. Nihon Rinsho *54*, 3309-3314.

Goodsell, D.S. (1999). The molecular perspective: methotrexate. Oncologist *4*, 340-341.

Gots, J.S., Benson, C.E., Jochimsen, B., and Koduri, K. (2009). Microbial models and regulatory elements in the control of purine metabolism. Paper presented at: Purine and pyrimidine metabolism: CIBA Foundation Symposium.

Halabe, A., and Sperling, O. (1994). Uric acid nephrolithiasis. Miner Electrolyte Metab *20*, 424-431.

Hammond, S.M., Bernstein, E., Beach, D., and Hannon, G.J. (2000). An RNA-directed nuclease mediates post-transcriptional gene silencing in Drosophila cells. Nature *404*, 293-296.

Han, D.D., Stein, D., and Stevens, L.M. (2000). Investigating the function of follicular subpopulations during Drosophila oogenesis through hormone-dependent enhancer-targeted cell ablation. Development *127*, 573-583.

Hediger, M.A., Johnson, R.J., Miyazaki, H., and Endou, H. (2005). Molecular physiology of urate transport. Physiology (Bethesda) *20*, 125-133.

Henderson, D.S. (2004). The chromosomes of Drosophila melanogaster. Methods Mol Biol *247*, 1-43.

Hirata, T., Cabrero, P., Berkholz, D.S., Bondeson, D.P., Ritman, E.L., Thompson, J.R., Dow, J.A., and Romero, M.F. (2012). In vivo Drosophilia genetic model for calcium oxalate nephrolithiasis. American Journal of Physiology-Renal Physiology *303*, F1555-F1562.

Hopkins, A.L. (2008). Network pharmacology: the next paradigm in drug discovery. Nature chemical biology *4*, 682-690.

JNIG (2002). Fly Stocks of the NIG: Strain 7171R-1 (Japanese National Institute of Genetics), pp.http://www.shigen.nig.ac.jp/fly/nigfly/rnaiFragmentDetailAction.do?input=irFragmentFullSeq&stockId=7171R-7171.

Johnson, R.J., Titte, S., Cade, J.R., Rideout, B.A., and Oliver, W.J. (2005). Uric acid, evolution and primitive cultures. Semin Nephrol *25*, 3-8.

Jurecka, A. (2009). Inborn errors of purine and pyrimidine metabolism. J Inherit Metab Dis *32*, 247-263.

Kanehisa, M., and Goto, S. (2000). KEGG: kyoto encyclopedia of genes and genomes. Nucleic acids research *28*, 27-30.

Ketting, R.F., Fischer, S.E., Bernstein, E., Sijen, T., Hannon, G.J., and Plasterk, R.H. (2001). Dicer functions in RNA interference and in synthesis of small RNA involved in developmental timing in C. elegans. Genes Dev *15*, 2654-2659.

Knauf, F., and Preisig, P.A. (2011). Drosophila: a fruitful model for calcium oxalate nephrolithiasis&quest. Kidney international *80*, 327-329.

Kratzer, J.T., Lanaspa, M.A., Murphy, M.N., Cicerchi, C., Graves, C.L., Tipton, P.A., Ortlund, E.A., Johnson, R.J., and Gaucher, E.A. (2014). Evolutionary history and metabolic insights of ancient mammalian uricases. Proc Natl Acad Sci U S A *111*, 3763-3768.

Laughon, A., Driscoll, R., Wills, N., and Gesteland, R.F. (1984). Identification of two proteins encoded by the Saccharomyces cerevisiae GAL4 gene. Mol Cell Biol *4*, 268-275.

Liebman, S.E., Taylor, J.G., and Bushinsky, D.A. (2007). Uric acid nephrolithiasis. Curr Rheumatol Rep *9*, 251-257.

Linton, S.M., and O'Donnell, M.J. (1999). Contributions of K+:Cl- cotransport and Na+/K+-ATPase to basolateral ion transport in malpighian tubules of Drosophila melanogaster. J Exp Biol *202*, 1561-1570.

Lotan, Y. (2009). Economics and cost of care of stone disease. Advances in chronic kidney disease *16*, 5-10.

Maalouf, N.M. (2014). Uric Acid Stones. Urinary Stones: Medical and Surgical Management, 26-35.

Mandal, M., Boese, B., Barrick, J.E., Winkler, W.C., and Breaker, R.R. (2003). Riboswitches control fundamental biochemical pathways in Bacillus subtilis and other bacteria. Cell *113*, 577-586.

Markstein, M., Dettorre, S., Cho, J., Neumuller, R.A., Craig-Muller, S., and Perrimon, N. (2014). Systematic screen of chemotherapeutics in Drosophila stem cell tumors. Proc Natl Acad Sci U S A *111*, 4530-4535.

Mathews, C.K.V.H., K.E. (1996). Nucleotide metabolism. In Biochemistry, Vol 2nd edn (Menlo Park, CA, USA.: Benjamin/Cummings Publishing Co., Inc.).

McCrudden, F.H. (2008). Uric Acid (BilioBazaar).

McGill, N.W., and Dieppe, P.A. (1991). The role of serum and synovial fluid components in the promotion of urate crystal formation. J Rheumatol *18*, 1042-1045.

Mendz, G.L., Shepley, A.J., Hazell, S.L., and Smith, M.A. (1997). Purine metabolism and the microaerophily of Helicobacter pylori. Archives of microbiology *168*, 448-456.

Miller, J., Chi, T., Kapahi, P., Kahn, A.J., Kim, M.S., Hirata, T., Romero, M.F., Dow, J.A., and Stoller, M.L. (2013). Drosophila melanogaster as an emerging translational model of human nephrolithiasis. The Journal of urology *190*, 1648-1656.

Muzyka, A., Tarkany, O., Yelizarov, V., and Boichuk, A. (1992-2005). Prism 4 for Windows (La Jolla, CA: GraphPad Softwere, Inc).

Nelson, D.L., and Cox, M.M. (2000). Lehninger Principles of Biochemistry (W. H. Freeman).

NTP (2015). Developmental Therapeutics Program, pp. http://dtp.nci.nih.gov/index.html.

Nudler, E., and Mironov, A.S. (2004). The riboswitch control of bacterial metabolism. Trends in biochemical sciences *29*, 11-17.

Oda, M., Satta, Y., Takenaka, O., and Takahata, N. (2002). Loss of urate oxidase activity in hominoids and its evolutionary implications. Mol Biol Evol *19*, 640-653.

Osterwalder, T., Yoon, K.S., White, B.H., and Keshishian, H. (2001). A conditional tissue-specific transgene expression system using inducible GAL4. Proc Natl Acad Sci U S A *98*, 12596-12601.

Parrish, S., Fleenor, J., Xu, S., Mello, C., and Fire, A. (2000). Functional anatomy of a dsRNA trigger: differential requirement for the two trigger strands in RNA interference. Mol Cell *6*, 1077-1087.

Preminger, G.M. (2007). Chapter 148: Stones in the Urinary Tract (Merck Sharp and Dohme Corporation: Whitehouse Station, New Jersey).

PubChem, N. (2015). National Center for Biotechnology Information: PubChem Compound Database (Bathesda, MD: National Library of Medicine), pp. http://www.ncbi.nlm.nih.gov/pccompound.

Rajagopalan, P.T., Zhang, Z., McCourt, L., Dwyer, M., Benkovic, S.J., and Hammes, G.G. (2002). Interaction of dihydrofolate reductase with methotrexate: ensemble and single-molecule kinetics. Proc Natl Acad Sci U S A *99*, 13481-13486.

Roman, G., Endo, K., Zong, L., and Davis, R.L. (2001). P[Switch], a system for spatial and temporal control of gene expression in Drosophila melanogaster. Proc Natl Acad Sci U S A *98*, 12602-12607.

Rosemeyer, H. (2004). The chemodiversity of purine as a constituent of natural products. Chem Biodivers *1*, 361-401.

Sarnesto, A., Linder, N., and Raivio, K.O. (1996). Organ distribution and molecular forms of human xanthine dehydrogenase/xanthine oxidase protein. Lab Invest *74*, 48-56.

Schlesinger, N. (2010). New agents for the treatment of gout and hyperuricemia: febuxostat, puricase, and beyond. Curr Rheumatol Rep *12*, 130-134.

Schmittgen, T.D., and Livak, K.J. (2008). Analyzing real-time PCR data by the comparative CT method. Nature protocols *3*, 1101-1108.

Simon, Z., Peragovics, Á., Vigh-Smeller, M., Csukly, G., Tombor, L., Yang, Z., Zahoránszky-Ko□halmi, G., Végner, L., Jelinek, B., and Hári, P. (2011). Drug effect prediction by polypharmacology-based interaction profiling. Journal of chemical information and modeling *52*, 134-145.

Simpson, M., Simpson, N., and Masheter, H. (1966). FLUFENAMIC ACID IN RHEUMATOID ARTHRITIS COMPARISON WITH ASPIRIN AND THE RESULTS OF EXTENDED TREATMENT. Rheumatology *8*, 208-213.

Singer, C., and Underwood, E.A. (1962). Short History of Medicine (New York and Oxford: Oxford University Press).

Sistare, F.D., and Haynes, R.C., Jr. (1985). The interaction between the cytosolic pyridine nucleotide redox potential and gluconeogenesis from lactate/pyruvate in isolated rat hepatocytes. Implications for investigations of hormone action. J Biol Chem *260*, 12748-12753.

Sorkhi, H., Hedaiati, F., and Bijani, A. (2011). Efficacy of Potassium Citrate Solution in Children with Urolithiasis. Journal of Babol University Of Medical Sciences *13*, 73-79.

Sriranganathan, M.K., Vinik, O., Bombardier, C., and Edwards, C.J. (2014). Interventions for tophi in gout. Cochrane Database Syst Rev *10*, CD010069.

St Pierre, S.E., Ponting, L., Stefancsik, R., and McQuilton, P. (2014). FlyBase 102--advanced approaches to interrogating FlyBase. Nucleic Acids Res *42*, D780-788.

Stamatelou, K.K., Francis, M.E., Jones, C.A., Nyberg, L.M., and Curhan, G.C. (2003). Time trends in reported prevalence of kidney stones in the United States: 1976-1994. Kidney Int *63*, 1817-1823.

Tatibana, M. (1996). [Mammalian phosphoribosylpyrophosphate synthetase]. Nihon Rinsho *54*, 3195-3201.

Tauc, H.M., Tasdogan, A., and Pandur, P. (2014). Isolating Intestinal Stem Cells from Adult Drosophila Midguts by FACS to Study Stem Cell Behavior During Aging. JoVE (Journal of Visualized Experiments), e52223-e52223.

Terkeltaub, R., Bushinsky, D.A., and Becker, M.A. (2006). Recent developments in our understanding of the renal basis of hyperuricemia and the development of novel antihyperuricemic therapeutics. Arthritis Res Ther *8 Suppl 1*, S4.

Trinchieri, A., Boccafoschi, C., Chisena, S., De Angelis, M., and Seveso, M. (1999a). [Study of the diuretic efficacy and tolerability of therapy with Rocchetta mineral water in patients with recurrent calcium kidney stones]. Arch Ital Urol Androl *71*, 121-124.

Trinchieri, A., Ostini, F., Nesopoli, R., Rovera, F., Montanari, E., and Zanetti, G. (1999b). A prospective study of recurrence rate and risk factors for recurrence after a first renal stone. The Journal of urology *162*, 27-30.

Walker, V., Stansbridge, E.M., and Griffin, D.G. (2013). Demography and biochemistry of 2800 patients from a renal stones clinic. Ann Clin Biochem *50*, 127-139.

Wallrath, L., Burnett, J., and Friedman, T. (1990). Molecular characterization of the Drosophila melanogaster urate oxidase gene, an ecdysone-repressible gene expressed only in the malpighian tubules. Molecular and cellular biology *10*, 5114-5127.

Wang, J., Kean, L., Yang, J., Allan, A.K., Davies, S.A., Herzyk, P., and Dow, J.A. (2004). Function-informed transcriptome analysis of Drosophila renal tubule. Genome Biol *5*, R69.

Wolf, S. (2014). Nephrolithiasis, pp. http://emedicine.medscape.com/article/437096-overview.

Wortmann, R.L., and Kelley, W.N. (2005). Gout and hyperuricemia, 7 edn (Philadelphia: Elsevier Saunders).

Wright, J.C., Lyons, M.M., Walker, D.G., Golomb, F.M., Gumport, S.L., and Medrek, T.J. (1964). Observations on the use of cancer chemotherapeutic agents in patients with mycosis fungoides. Cancer *17*, 1045-1062.

Wu, X., Wakamiya, M., Vaishnav, S., Geske, R., Montgomery, C., Jr., Jones, P., Bradley, A., and Caskey, C.T. (1994). Hyperuricemia and urate nephropathy in urate oxidase-deficient mice. Proc Natl Acad Sci U S A *91*, 742-746.

Yalkowsky, S.H., and He, Y. (2003). Handbook of Aqueous Solubility Data: An Extensive Compilation of Aqueous Solubility Data for Organic Compounds Extracted from the AQUASOL dATAbASE (Boca Raton, FL: CRC Press LLC).

Yamada, Y., Nomura, N., Yamada, K., Kimura, R., Fukushi, D., Wakamatsu, N., Matsuda, Y., Yamauchi, T., Ueda, T., Hasegawa, H.*, et al.* (2014). Hypoxanthine guanine phosphoribosyltransferase (HPRT) deficiencies: HPRT1 mutations in new Japanese families and PRPP concentration. Nucleosides Nucleotides Nucleic Acids *33*, 218-222.

Yamada, Y., Yamada, K., Nomura, N., Yamano, A., Kimura, R., Tomida, S., Naiki, M., and Wakamatsu, N. (2010). Molecular analysis of two enzyme genes, HPRT1 and PRPS1, causing X-linked inborn errors of purine metabolism. Nucleosides Nucleotides Nucleic Acids *29*, 291-294.

Zamore, P.D., Tuschl, T., Sharp, P.A., and Bartel, D.P. (2000). RNAi: double-stranded RNA directs the ATP-dependent cleavage of mRNA at 21 to 23 nucleotide intervals. Cell *101*, 25-33.

Zhang, F., Zhao, Y., and Han, Z. (2013). An in vivo functional analysis system for renal gene discovery in Drosophila pericardial nephrocytes. J Am Soc Nephrol *24*, 191-197.

Zhu, Y., Pandya, B.J., and Choi, H.K. (2011). Prevalence of gout and hyperuricemia in the US general population: the National Health and Nutrition Examination Survey 2007-2008. Arthritis Rheum *63*, 3136-3141.

11 Tables and Figures

11.1 Tables

Table 1: Bacto yeast extract composition
The composition of Bacto yeast extract from manufactures brochure. Table adapted from (BD-Bioscience, 2006).

	Total Nitrogen (%)	Amino Nitrogen (%)	Amino Nitrogen/Total Nitrogen	Total Carbohydrate (mg/g)
Yeast Extract, Bacto	10.9	6	0.55	163.3

Table 2: Table of Primers Used
The table shown contains forward and reverse primers for UO and β-Tubulin 56D RA. Primers where designed using BLAST (Altschul et al., 1997).

	Forward Primer	Reverse Primer
UO	GCGATGTGGTTATAAGGAGAACA	TCTTCAGCACCCGGAGAC
β-Tubulin 56D RA	AGAAAGCCTTGCGCCTGAACA	ACATCCGGCCCCGTGGTC

11.2 Figures

Figure 1: Purine Structure
Purine skeleton with numbering pattern for atoms of the fused pyrimidine ring (1-6) and imidazole ring (4-5, 7-9). Picture adapted from NCBI PubChem Compound Database, CID: 1044 (PubChem, 2015).

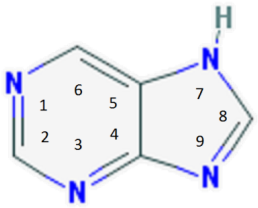

Figure 2: Adenine and Guanine Structure
Purines: adenine (left) and guanine (right). Picture adapted from NCBI PubChem Compound Database, CID: 190 & 764 (PubChem, 2015).

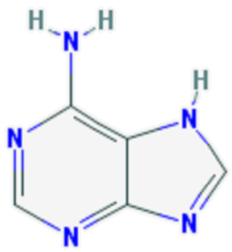

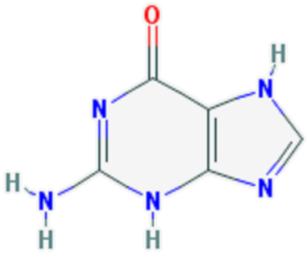

Figure 3: ATP Structure
The molecule shown is ATP. Picture adapted from NCBI PubChem Compound Database, CID: 5957 (PubChem, 2015).

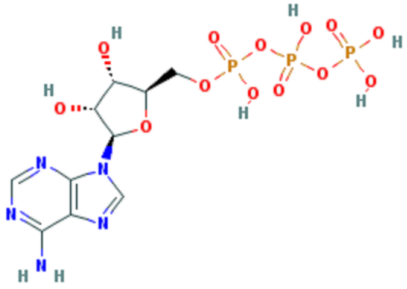

Figure 4: NADH structure
Picture adapted from NCBI PubChem Compound Database, CID: 439153 (PubChem, 2015).

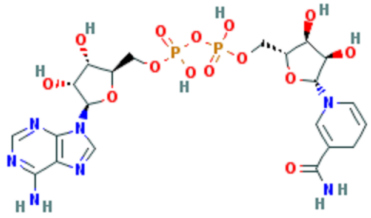

Figure 5: Xanthine Structure
Picture adapted from NCBI PubChem Compound Database, CID: 1188 (PubChem, 2015).

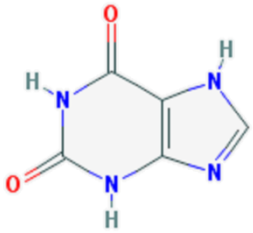

Figure 6: Purine degradation pathway in flies and humans (excluding urate oxidase and allantoin)
Pictured is the purine degradation pathway from major metabolic nucleotides AMP, IMP, and GMP to uric acid (Mathews, 1996).

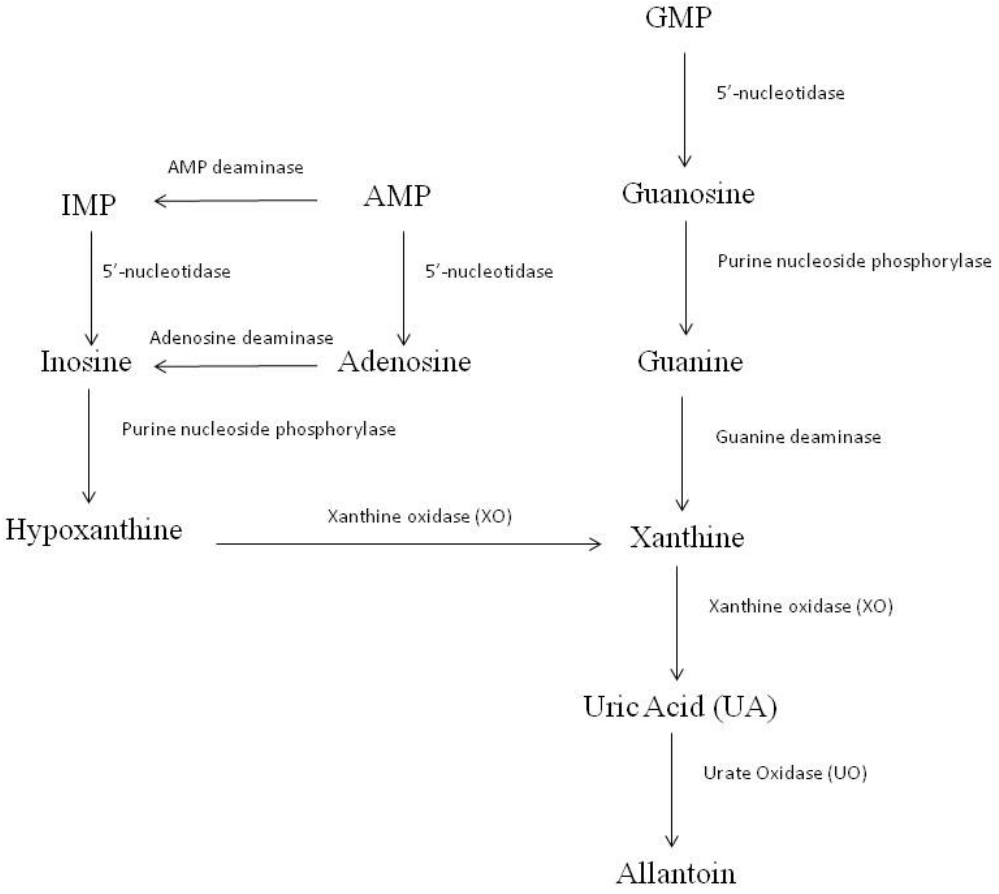

Figure 7: Uric acid and urate anion interconversion
Picture adapted from (Hediger et al., 2005).

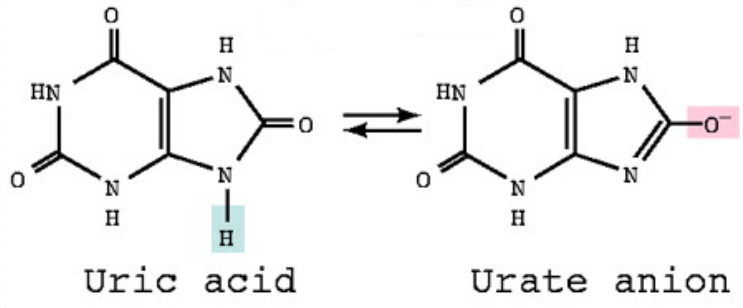

Figure 8: Allantoin structure
Picture adapted from NCBI PubChem Compound Database, CID: 204 (PubChem, 2015).

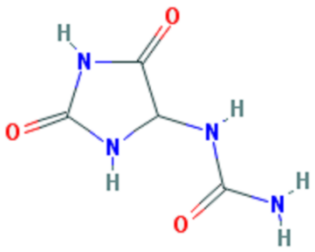

Figure 9: PCR Targets Transcripts

UO: *Urate Oxidase* Common Gene 7171 (CG7171) sequence from BLAST database (Altschul et al., 1997).

5'-
ATCAGTATCAAAGTGAGAGTGATTGCAGTCACAATGTTTGCCACGCCCCTCAGACAGCCAGCTGCGGCTA
ACCACCAGACCCCAAAGAATTCCGCCGGCATGGATGAGCATGGTAAGCCGTATCAGTACGAGATTACCG
ATCACGGATACGGCAAGGATGCGGTCAAGGTGCTGCATGTCAGCCGCAACGGACCCGTGCACGCCATCC
AGGAATTCGAGGTGGGCACTCACCTGAAGTTGTACAGCAAAAAGGATTACTACCAGGGCAACAACTCGG
ACATCGTGGCCACCGATTCGCAGAAGAACACCGTCTATTTGCTGGCGAAAAAGCATGGCATTGAAAGTCC
CGAGAAGTTTGCTCTGCTCCTGGCCAGGCACTTTATTAACAAATACTCGCACGTGGAGGAGGCGCACGTT
CATGTGGAGGCGTATCCCTGGCAGCGAGTTTGCCAGGAGGAGACCAGGACCAACGTCAATGGGAAGTGC
GAGAACGGAGTCCAAGGGAACTGCGACTTCAGCTCCATTGACAACAGATCACTGCACAATCACGCTTTTA
TATTCACGCCCACCGCTCTTCACTACTGCGATGTGGTTATAAGGAGAACAGATCCCAAACAAACGGTCAT
CACGGGCATCAAGGGTCTCCGGGTGCTGAAGACGACCCAATCCTCGTTCGTGAACTTCGTGAACGATGAG
TTCAGATCTCTGCCAGATCAGTATGATCGCATCTTTAGCACCGTGGTGGATTGCTCCTGGGAGTACTCCGA
TACCGAGAACTTGGACTTCCTCAGGGCCTGGCAAACGGTCAAAAACATAATCATTCGTAACTTTGCTGGC
GATCCGCAGGTGGGCGTGTCCTCGCCCTCCGTTCAGCACACCCTGTATCTGAGTGAAAGACAGGTCCTGG
ATGTCCTGCCGCAGGTGTCGGTCATTTCGATGACCATGCCAAACAAGCACTACTTCAACTTCGATACGAA
GCCCTTCCAGAAGATTGCACCCGGCGACAACAATGAAGTTTTCATCCCAGTGGACAAGCCACATGGCACC
ATCTATGCCCAATTGGCCCGGAAGAACATCAATAGTCACCTGTAGATCGATCTCTGATGTAGTAAATCTA
AATCAATCTAAATCAATTTAGCCAATTCATAATTGCATGCGGCGAAGTTATATATGTATTTTAAATTATTT
AAGCAAACGAATCATATGCTGCGTTCTTCTTATTTAAACAATAATAAACTAATAAAAAATAAAGTGTAAA
AATG-3'

Tubuling 56D RA: Common Gene 9277 (CG9277) sequence from BLAST database (Altschul et al., 1997).

5'-
ATAGTAGTTATACAGCTCAGTTCCAGCCCACGCCCGAAGATTCGAGTAAGATCGGTCGGCGGAACGCAAT
GACAGCTGCGCCTCGAGATCCGAAACGAAAACCCACGCCAGATGACGTTATCGTTGGTGTGGCGATGGT
GCTGCTGGTCGTGGTGGTGGAAACGCACCAAAAATGGCAGCGAATAAGTTATGTTAATCGGAGCTCGGC
CCATACACAGAGTTTATGATGGCGTACATGGGTGGCCTAAACCACGTAGCCGAGCCCAGACATGTTTCTG
GGAGATCATCTCCGATGAGCATGGCATCGATGCCACCGGCGCCTACCACGGTGACAGCGACCTGCAGCT
GGAGCGCATCAATGTGTACTACAATGAGGCGTCCGGTGGCAAGTACGTGCCCCGCGCTGTCCTTGTCGAT
CTGGAGCCCGGCACCATGGACTCTGTGCGATCGGGACCTTTCGGCCAGATCTTCAGGCCCGACAACTTTG
TGTTCGGCCAGTCGGGTGCCGGCAACAACTGGGCCAAGGGTCATTACACAGAGGGTGCTGAGCTGGTGG
ACTCAGTGCTCGATGTTGTCCGCAAGGAGGCCGAATCCTGCGACTGCCTGCAAGGCTTCCAACTCACACA
CTCCCTTGGCGGCGGCACTGGCTCCGGTATGGGAACCCTGCTGATTTCCAAGATCCGCGAGGAGTACCCC
GACAGGATCATGAACACATACTCGGTTGTGCCGTCGCCCAAGGTGTCGGACACCGTTGTGGAGCCCTACA
ACGCCACCCTGTCGGTGCACCAGCTGGTCGAGAACACGGACGAGACCTACTGCATCGACAACGAGGCTC
TCTACGATATCTGCTTCCGCACCCTCAAGCTGACGACACCCACATACGGTGACCTGAACCATCTTGTCTCC
CTGACCATGTCCGGCGTAACCACCTGCCTCCGATTCCCCGGCCAACTGAACGCTGATCTCCGCAAGCTGG
CCGTCAACATGGTGCCCTTCCCACGTCTTCACTTCTTCATGCCCGGCTTCGCTCCCCTGACCTCCCGAGGA

TCCCAGCAGTACCGCGCCCTCACCGTGCCCGAGCTGACCCAGCAGATGTTCGATGCCAAGAACATGATGG
CCGCCTGCGACCCACGCCACGGACGCTACCTTACCGTCGCCGCCATCTTCCGTGGACGCATGTCCATGAA
GGAGGTCGACGAGCAGATGCTGAACATCCAGAACAAGAACAGCTCCTACTTCGTCGAATGGATCCCCAA
CAACGTGAAGACCGCCGTGTGCGACATCCCGCCCCGTGGTCTGAAGATGTCCGCCACCTTCATCGGCAAC
TCCACTGCCATCCAGGAGCTGTTCAAGCGCATCTCCGAGCAGTTCACCGCTATGTTCAGGCGCAAGGCTT
TCTTGCATTGGTACACCGGCGAGGGCATGGACGAGATGGAGTTCACCGAGGCCGAGAGCAACATGAACG
ATCTGGTGTCCGAGTACCAGCAGTACCAGGAGGCCACCGCCGACGAGGACGCCGAGTTCGAGGAGGAGC
AGGAGGCTGAGGTCGACGAGAACTAAATTCGAATCGGAAATCAATCGAATTCTCGATCAATGTTTTGCGA
AAAAAAATGAAACGAGAACAAATGAATTCAGTTGTAAAAGATTTGTTCTCTTAACAACGTAATCAATAA
AGTCGGATCCAATTTTGTTCACAAGTCT-3’

Figure 10: Genome of *UO RNAi* Line
Shown is the genome sequence of *UO RNAi* line on the left of arm of the 2nd chromosome.

DNA sequence of *UO RNAi* line:
5’-
AACCACCAGACCCCAAAGAATTCCGCCGGCATGGATGAGCATGGTAAGCCGTATCAGTACGAGATTACC
GATCACGGATACGGCAAGGATGCGGTCAAGGTGCTGCATGTCAGCCGCAACGGACCCGTGCACGCCATC
CAGGAATTCGAGGTGGGCACTCACCTGAAGTTGTACAGCAAAAAGGATTACTACCAGGGCAACAACTCG
GACATCGTGGCCACCGATTCGCAGAAGAACACCGTCTATTTGCTGGCGAAAAAGCATGGCATTGAAAGT
CCCGAGAAGTTTGCTCTGCTCCTGGCCAGGCACTTTATTAACAAATACTCGCACGTGGAGGAGGCGCACG
TTCATGTGGAGGCGTATNCCCTGGCAGCGAGTTTGCCAGGAGGAGACCAGGACCAACGTCAATGGGAAG
TGCGAGAACGGAGTCCAAGGGAACTGCGACTTCAGCTCCATTGACAACAGATCACTGCACAATCACGCT
TTTATATTCACGCCCAC-3’

W1118 Line
The *W1118* strain is a wild type strain that serves as a genetic control and is homozygous for wild type alleles. Fly strain was acquired from the Benz Lab at Caltech Institute of Technology, Pasadena, CA.

Da Driver Line
The *Da* Driver Line contains homozygous Gal4 transcription factors downstream of promoters for Da protein. The Da protein is ubiquitously expressed throughout development and at moderate levels throughout the body of the fly (St Pierre et al., 2014). Fly strain was acquired from the Benz Lab at Caltech Institute of Technology, Pasadena, CA.

Figure 11: qRT-PCR of urate oxidase mRNA confirms efficient knockdown using RNAi in *D. melanogaster*

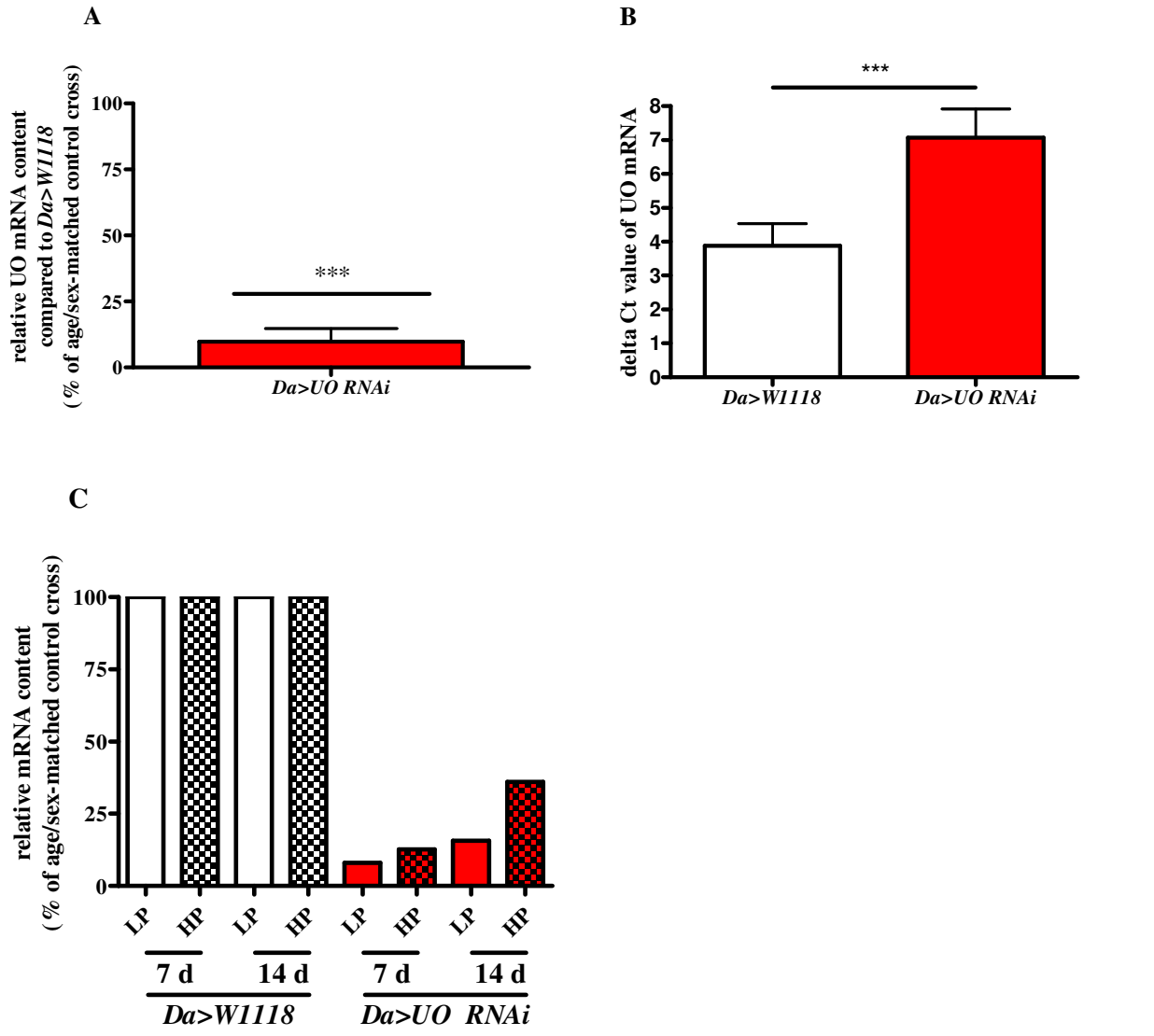

(A) qRT - PCR of urate oxidase mRNA transcripts of *Da > UO RNAi* (urate oxidase knockdown) flies fed the stock diet until 0 d relative to *Da > W1118*, control flies fed the stock diet until 0 d. Tubulin 56D RA was used as loading control for ΔC_t comparison. Shown is the $\Delta\Delta C_t$ of UO KD (red bar) compared to *Da > W1118* (not shown). Student's two-tailed t-test was performed on the $\Delta\Delta C_t$, *** = $p < 0.001$. Error bar represents 95% CI. Biological n = 11. For each biological n, 10 flies were sacrificed.

(B) ΔC_t values from (A) of *Da > UO RNAi* (urate oxidase knockdown) flies fed the stock diet until 0 d relative to *Da > W1118*, control flies fed the stock diet until 0 d. Tubulin 56D RA was used as loading control for ΔC_t comparison. Student's two-tailed t-test was performed on the ΔC_t, *** = $p < 0.001$. Error bar represents 95% CI. Biological n = 11. For each biological n, 10 flies were sacrificed.

(C) qRT - PCR of urate oxidase mRNA transcripts of *Da > UO RNAi* (urate oxidase knockdown) flies fed the LP (non-checkered bars) and HP (checkered bars) diets after 7, and 14 d versus *Da > W1118,* control flies fed the LP and HP diets until 7 d and 14 d. Tubulin 56D RA was used as loading control for ΔC_t comparison. Shown is the $\Delta\Delta C_t$ of urate oxidase knockdown (red bars) compared to *Da > W1118* (white bars) flies. Biological n = 1. For each biological n, 10 flies were sacrificed.

Figure 12: Uric acid levels increased with urate oxidase knockdown on the high purine diet in *D. melanogaster*

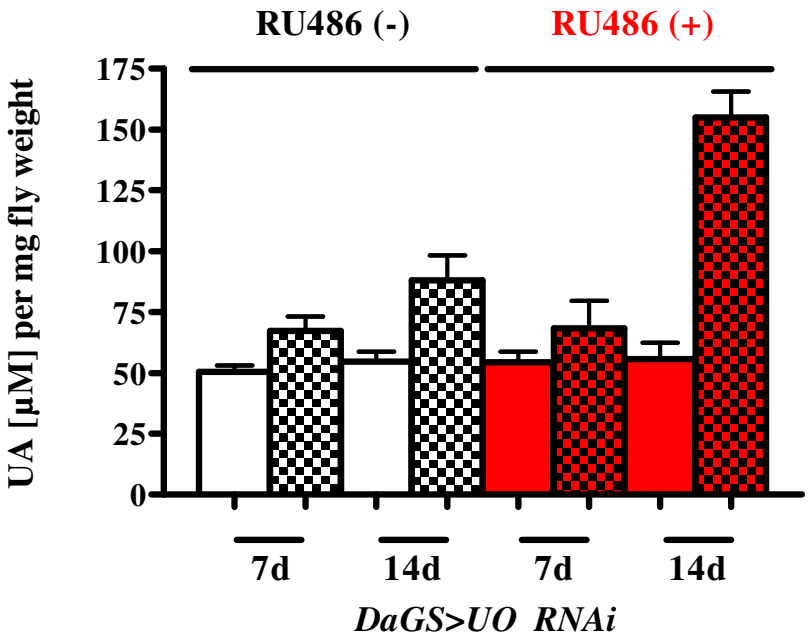

Uric acid levels of *DaGS > UO RNAi* (urate oxidase knockdown) flies fed the LP (+) and HP (+) diets (red bars), after 7 d and 14 d versus *DaGS > UO RNAi* (control) flies fed the LP (-) and HP (-) diets (white bars) after 7 d and 14 d (biological n = 3). For each biological n, 5 flies were sacrificed. Measurements were standardized to the average weight of 5 flies. UA = Uric Acid, RU486 (-) = null for urate oxidase knockdown, RU486 (+) = urate oxidase knockdown.

Figure 13: Uric acid kidney stone formation in *D. melanogaster* was induced by urate oxidase knockdown and dietary purine supplementation

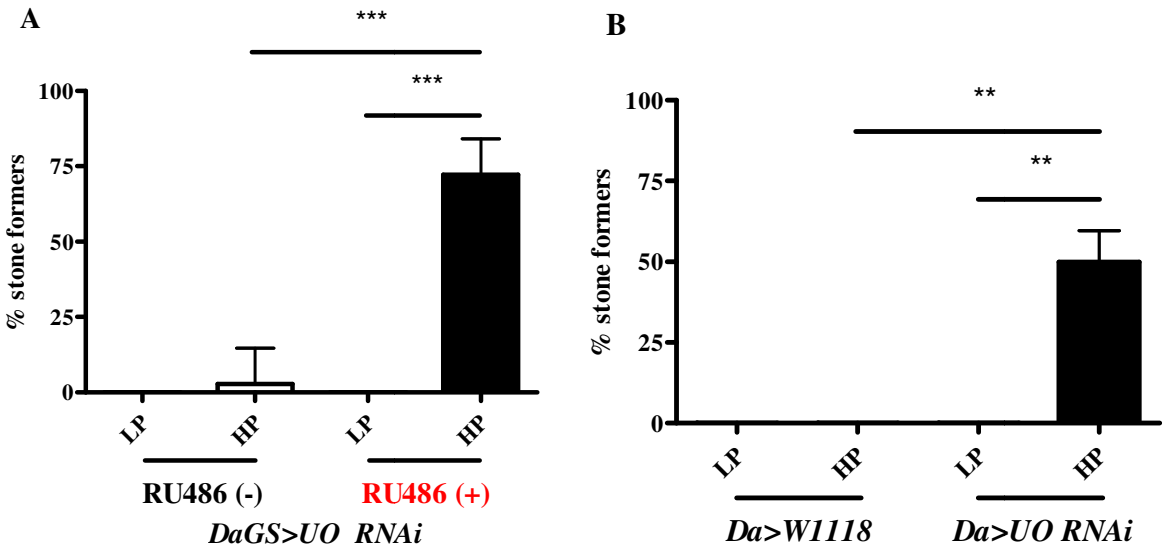

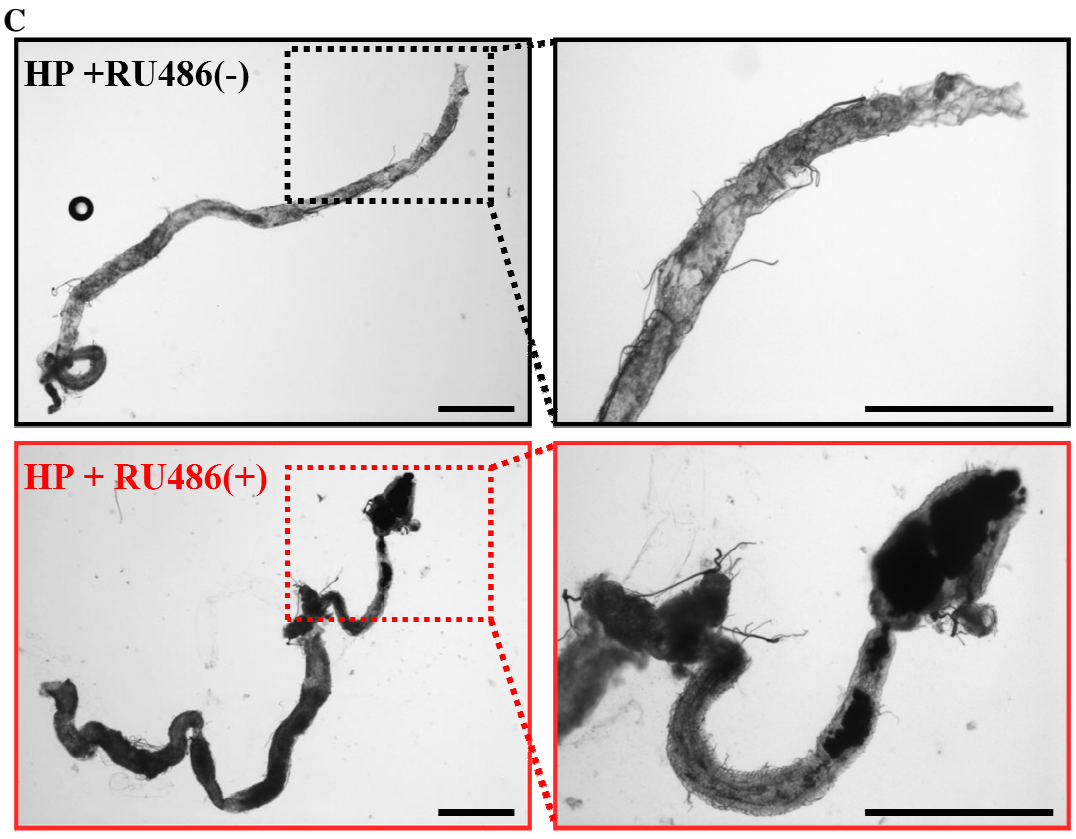

(A) Uric acid kidney stone formation in *DaGS > UO RNAi* (urate oxidase knockdown) flies fed the LP (+) (white bar) and HP (+) diets (black bar) versus *DaGS >UO RNAi* (control) flies fed the LP (-) (grey bar) and HP (-) (grey checkered bar) diets

after 14 d (biological n = 3). For each biological n, 12 flies were sacrificed and dissected. One-way ANOVA was performed on uric acid kidney stone formation, *** = $p < 0.05$. Error bar represents 95% CI.

(B) Uric acid kidney stone formation in *Da > UO RNAi* (uric oxidase knockdown) flies fed the LP (white bar) and HP (black bar) diets versus *Da > W1118* (control) flies fed the LP (grey bar) and HP (grey checkered bar) diets after 14 d (biological n = 3). For each biological n, 12 flies were sacrificed and dissected. One-way ANOVA was performed on uric acid kidney stone formation, ** = $p < 0.01$. Error bar represents 95% CI.

(C) Representative images from (Fig. 13A) taken of dissected guts from *DaGS >UO RNAi* (urate oxidase knockdown) flies fed the HP (+) diet (red box) versus *DaGS > UO RNAi* (control) flies fed the HP (-) diet (black box). Black bar represents a length of 500 µm.

Figure 14: Allopurinol and potassium citrate supplementation reduced uric acid kidney stone formation when urate oxidase was knocked down and dietary purine supplemented

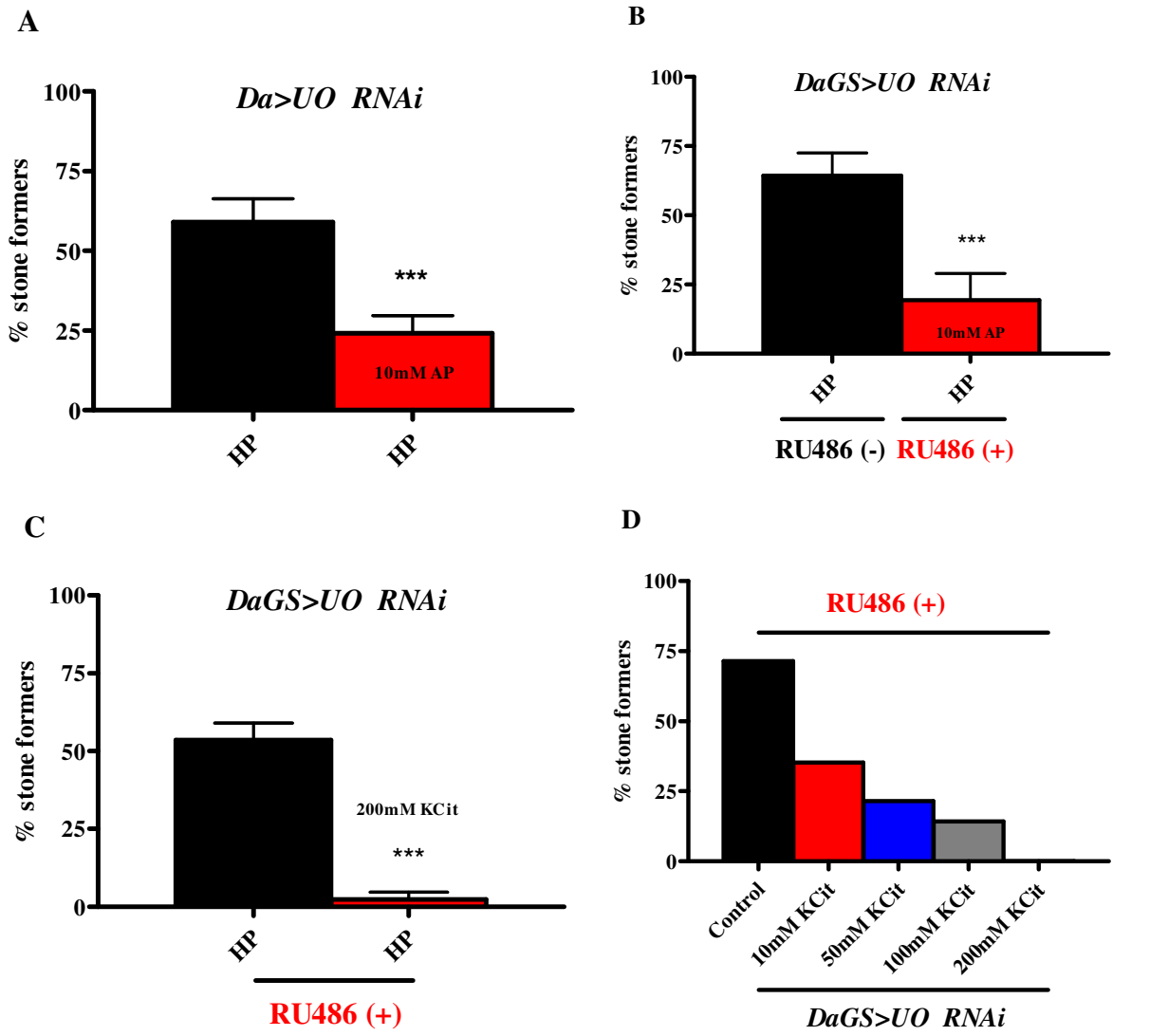

(A) Uric acid kidney stone formation in *Da > UO RNAi* (urate oxidase knockdown) flies fed the HP diet (black bar) versus *Da > UO RNAi* flies fed the HP diet supplemented with 10 µM allopurinol (red bar) after 14 d (biological n = 3). For each biological n, 12 flies were sacrificed and dissected. *** = $p < 0.001$. Error bar represents 95% CI. AP = Allopurinol.

(B) Uric acid kidney stone formation in *DaGS > UO RNAi* (urate oxidase knockdown) flies fed the HP (+) diet (black bar) versus *DaGS > UO RNAi* flies fed the HP (+) diet supplemented with 10 µM allopurinol (red bar) after 14 d using micro-

dissection (biological n = 3). For each biological n, 12 flies were sacrificed and dissected. *** = $p < 0.001$. Error bar represents 95% CI. AP = Allopurinol.

(C) Uric acid kidney stone formation in *DaGS > UO RNAi* (urate oxidase knockdown) flies fed the HP (+) diet (black bar) versus *DaGS > UO RNAi* flies fed the HP (+) diet supplemented with 200 mM potassium citrate (red bar) after 14 d (biological n = 3). For each biological n, 12 flies were sacrificed and dissected. *** = $p < 0.001$. Error bar represents 95% CI. KCit = Potassium Citrate.

(D) Uric acid kidney stone formation in *DaGS > UO RNAi* (urate oxidase knockdown) flies fed the HP (+) diet (black bar) and HP (+) diet supplemented with 10 mM potassium citrate (red bar), 50 mM potassium citrate, 100 mM potassium citrate, and 200 mM potassium citrate after 14 d (biological n = 1). For each biological n, 12 flies were sacrificed and dissected.

Figure 15: Methotrexate, hydrochlorothiazide, and l-lysine supplementation reduced uric acid kidney stone formation when urate oxidase was knocked down and dietary purine supplemented

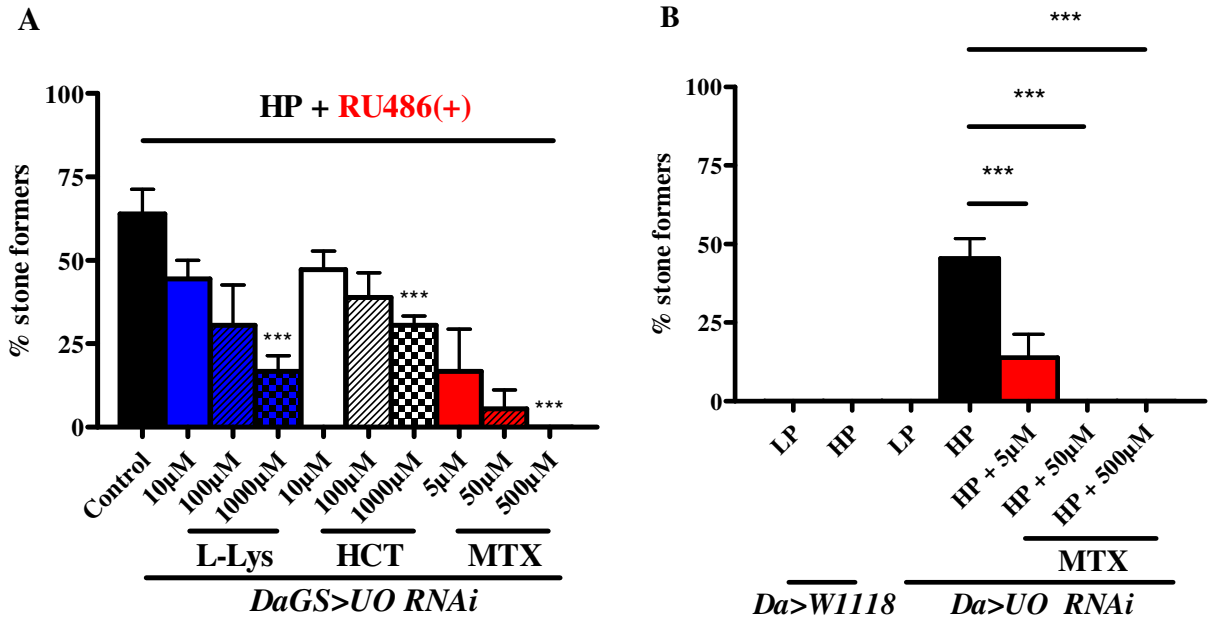

(A) Uric acid kidney stone formation in *DaGS > UO RNAi* (urate oxidase knockdown) flies fed the HP (+) diets supplemented with 10 μM (non-black solid bars), 100 μM (stripped bars), and 1000 μM (checkered bars) l-lysine (blue bars), hydrochlorothiazide (white bars), and methotrexate (red bars) versus *DaGS > UO RNAi* (control) flies fed the HP (-) diet (black bar) after 14 d (biological n = 3). For each biological n, 12 flies were sacrificed and dissected. *** = $p < 0.001$. Error bar represents 95% CI. L-Lys = l-lysine, HCT = hydrochlorothiazide, and MTX = methotrexate.

(B) Uric acid kidney stone formation in *Da > UO RNAi* (urate oxidase knockdown) flies fed the LP diet (white bar), HP diet (black bar), HP diet supplemented with 5 μM (red solid bar), 50 μM methotrexate (red stripped bar), and 500 μM methotrexate versus *Da >W*, control flies fed the LP (grey bar) and HP (grey checkered bar) diet after 14 d (biological n = 3). For each biological n, 12 flies were sacrificed and dissected. *** = $p < 0.001$. Error bar represents 95% CI. MTX = methotrexate.

Figure 16: Possible mechanisms by which allopurinol, potassium citrate, l-lysine, and methotrexate reduced uric acid kidney stone formation

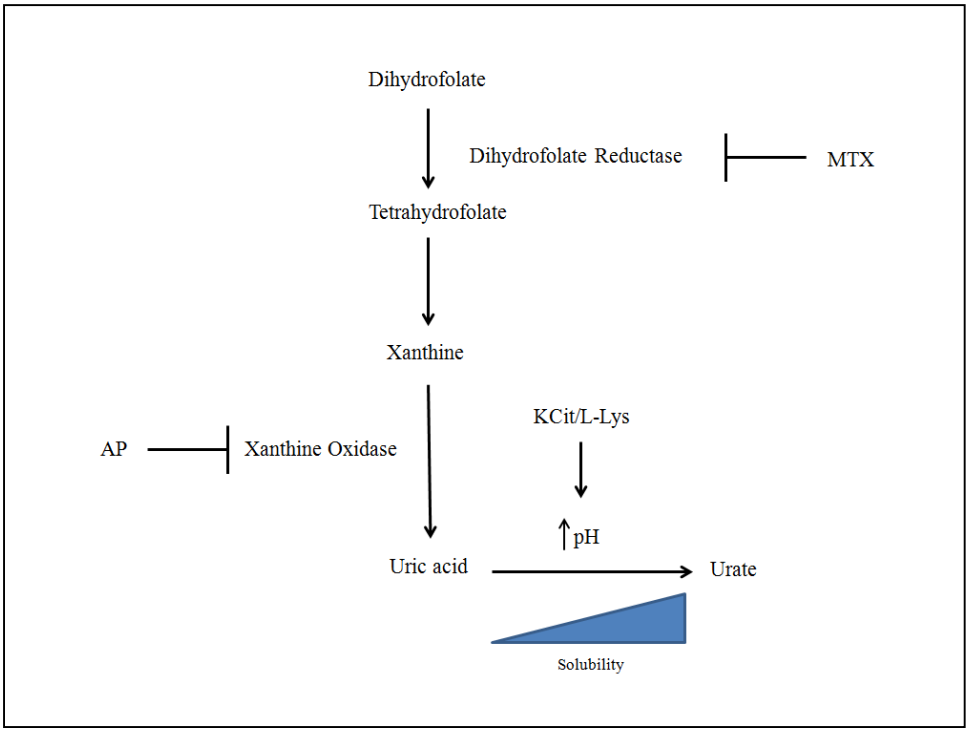

A simplified overview of purine metabolism with homologous components between *D. melanogaster* and humans and the possible mechanisms by which, AP=Allopurinol, KCit=Potassium Citrate, L-Lys = L-Lysine, and MTX = Methotrexate reduces uric acid and uric acid kidney stones. Allopurinol inhibits xanthine oxidase, the enzyme that converts xanthine into uric acid. Potassium citrate alkalizes and increases the pH of urine, which drives the formation of more soluble urate. L-lysine is also an alkalizer and increases the pH of urine, which drives the formation of more soluble urate. Methotrexate, an inhibitor of dihydrofolate reductase, prevents the essential conversion of dihydrofolate into tetrahydrofolate for purine synthesis, thus reducing the purine load and subsequently reducing uric acid and uric acid kidney stone formation.

Figure 17: Possible mechanisms by which hydrochlorothiazide reduced uric acid kidney stone formation

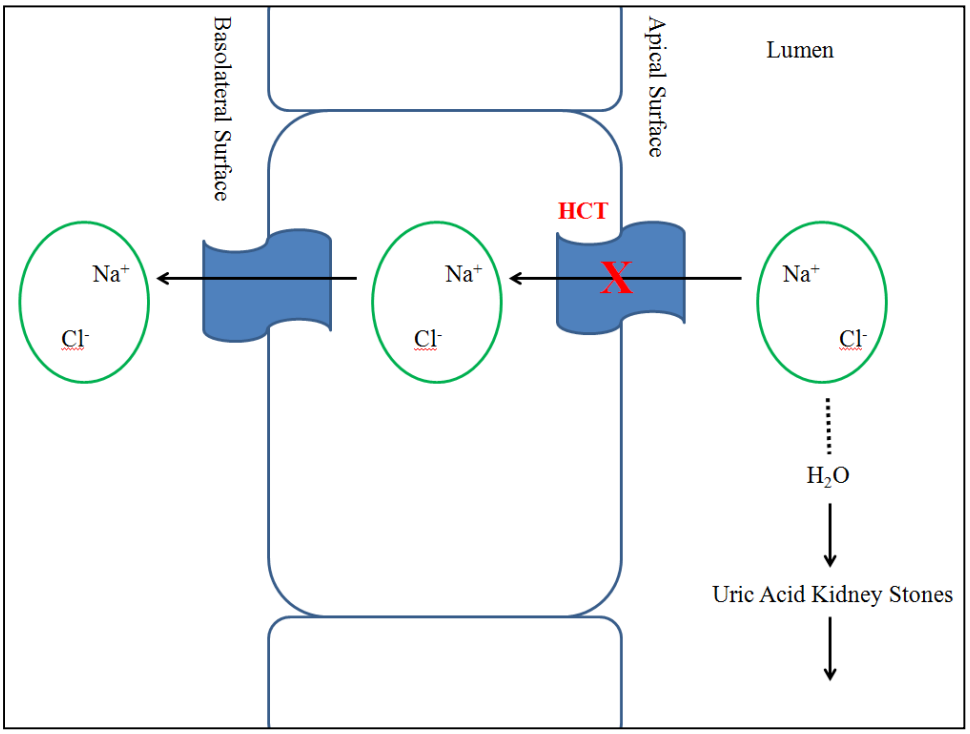

A diagram of basolateral cells of the human nephron and *D. melanogaster* malpighian tubules and the possible mechanism by which inhibition of Na^+Cl^- co-transporter by hydrochlorothiazide increases urine output and reduces uric acid kidney stone formation. Na^+Cl^- co-transporters facilitate the movement of Na^+ and Cl^-, creating an osmotic gradient that causes the passive movement of water from the lumen to basolateral side. Inhibition of Na^+Cl^- co-transporters prevents the movement of Na^+ and subsequently water from the lumen to the basolateral side, which increases in urine volume. The increased urine volume causes the expulsion of small and medium sized stones. HCT = Hydrochlorothiazide.

Figure 18: Seven Inhibitors and six enhancers of uric acid kidney stone formation were found in a medium throughput screen of 117 compounds

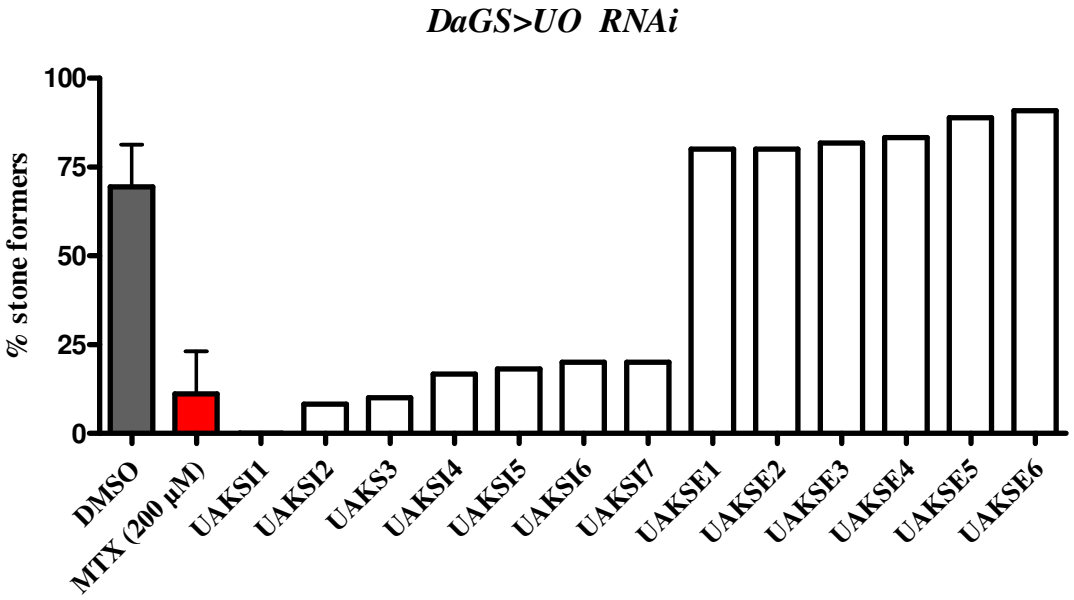

Inhibitors (< 20% stone formers) and enhancer (> 20 % stone formers) from medium throughput screen of 117 compounds. Uric acid kidney stone formation in *DaGS > UO RNAi* (urate oxidase knockdown) flies fed the HP (+) diet supplemented with synthetic purines (adenine = 10 mM and guanine = 10mM) and topped with 1:50 dimethyl sulfoxide solution (reference control, n = 3, grey bar), the HP (+) diet supplemented synthetic purines and topped with 200 µM of MTX (n = 3, red bar) in 1:50 dimethyl sulfoxide solution (positive control, red bar), and the HP (+) diet supplemented synthetic purines and topped with compounds dissolved in 1:50 dimethyl sulfoxide from the 117 compound library (n=1). For each biological n, 6-15 flies were sacrificed and dissected. MTX = methotrexate. DMSO = dimethyl sulfoxide.

12 Appendix

12.1 Original Data

Figure 19: Original Data

Figure	Exp. ID/Date	Assay	Cross	0d Values	7d Values	14d Values
Fig. 11A						
	130607	qRT-PCR, delta delta Ct Value		6%		
	130607(repeat)			5%		
	130710			7%		
	130717			4%		
	130725			4%		
	130830			7%		
	130920			5%		
	131007			20%		
	131025			26%		
	140117			12%		
	140124			13%		
Fig. 11B						
	130607	qRT-PCR, delta Ct	Da>W1118	2.8867		
	130607(repeat)			3.0137		
	130710			4.3433		
	130717			3.49		
	130725			3.8233		
	130830			5.9133		
	130920			4.1167		
	131007			4.4233		
	131025			4.3567		
	140117			2.2467		
	140124			4.1033		
	130607		Da>UO RNAi	6.6567		
	130607(repeat)			6.1967		
	130710			9.0333		
	130717			7.9967		
	130725			6.2467		
	130830			8.62		
	130920			8.3333		
	131007			6.7767		
	131025			5.5933		
	140117			5.2433		

	140124			7.0567		
Fig. 11C						
	131121	qRT-PCR, delta delta Ct Value	Da>W1118		LP replicate 1=100%	LP replicate 1=100%
					LP replicate 2=100%	LP replicate 2=100%
					LP replicate 3=100%	LP replicate 3=100%
					HP replicate 1=100%	HP replicate 1=100%
					HP replicate 2=100%	HP replicate 2=100%
					HP replicate3=100%	HP replicate3=100%
			Da>UO RNAi		LP replicate 1=7%	LP replicate 1=12%
					LP replicate 2=8%	LP replicate 2=15%
					LP replicate 3=9%	LP replicate 3=20%
					HP replicate 1=14%	HP replicate 1=34%
					HP replicate 2=12%	HP replicate 2=38%
					HP replicate3=12%	HP replicate3=36%
Fig. 12						
	141113	Uric Acid (uM per mg of fly weight)	DaGS>UO RNAi		LP(-)=54 µM/mg	LP(-)=61 µM/mg
					LP(+)=62 µM/mg	LP(+)=69 µM/mg
					HP(-)=68 µM/mg	HP(-)=80 µM/mg
					HP(+)=108 µM/mg	HP(+)=176 µM/mg
	150202	Uric Acid (uM per mg of fly weight)	DaGS>UO RNAi		LP(-)=52 µM/mg	LP(-)=46 µM/mg
					LP(+)=54 µM/mg	LP(+)=49 µM/mg
					HP(-)=77 µM/mg	HP(-)=46 µM/mg
					HP(+)=82 µM/mg	HP(+)=146 µM/mg
	150224	Uric Acid (uM per mg of fly weight)	DaGS>UO RNAi		LP(-)=45 µM/mg	LP(-)=56 µM/mg
					LP(+)=48 µM/mg	LP(+)=49 µM/mg
					HP(-)=57 µM/mg	HP(-)=79 µM/mg
					HP(+)=74 µM/mg	HP(+)=143 µM/mg
Fig. 13A						
	150217	Dissections	Da>W1118			LP=0%,0/12
						HP=0%,0/12
	150217	Dissections	Da>UO RNAi			LP=0%,0/12
						HP=50.0%,6/12
	150219	Dissections	Da>W1118			LP=0%,0/12
						HP=0%,0/12
	150219	Dissections	Da>UO RNAi			LP=0%,0/12
						HP=66..7%,7/12
	140610	Dissections	Da>W1118			LP=0%, 0/12
						HP=0%,0/12
	140610	Dissections	Da>UO RNAi			LP=0%, 0/12
						HP=33.3%,4/12
Fig. 13B						
	140922	Dissections	DaGS>UO RNAi			LP(-)=0%,0/12
						LP(+)=0%,0/12

						HP(-) = 0%,0/12
						HP(-) = 75%,9/12
	140905	Dissections	DaGS>UO RNAi			LP(-)=0%,0/12
						LP(+)=0%,0/12
						HP(-) = 8.3%,1/12
						HP(-) = 66.7%8/12
	140912	Dissections	DaGS>UO RNAi			LP(-)=0%,0/12
						LP(+)=0%,0/12
						HP(-) = 0%,0/12
						HP(-) = 75%9/12
Fig. 14A						
	140320	Dissections	Da>W1118			HP=0%,0/12
			Da>UO RNAi			HP=75.0%,9/12
						HP+AP(10mM)=16.7%,2/12
	150217	Dissections	Da>W1118			HP=0%,0/12
			Da>UO RNAi			HP=50.0%,6/12
						HP+AP(10mM)=33.3%4/12
	150219	Dissections	Da>W1118			HP=0%
			Da>UO RNAi			HP=66.7%
						HP+AP(10mM)=25.0%
Fig. 14B						
	150122	Dissections	DaGS>UO RNAi			HP(-)=8.3%,1/12
						HP(+)=75.0%,9/12
						HP(+)+AP(10mM)=0.0%,0/12
	150213	Dissections	DaGS>UO RNAi			HP(-)=0.0%,0/12
						HP(+)=50.0%
						HP(+) + AP(10mM)=33.3%,4/12
	150215	Dissections	DaGS>UO RNAi			HP(-)=8.30%,1/12
						HP(+)=66.7%,9/12
						HP(+) + AP(10mM)=25.0%,3/12
Fig. 14C						
	141119	Dissections	DaGS>UO RNAi			HP(-)=8.30%,1/12
						HP(+)=50.0%,6/12
						HP(+) + Kcit(200mM) = 0.0%
	150213	Dissections	DaGS>UO RNAi			HP(-)=0.0%
						HP(+)=50.0%
						HP(+) + Kcit(200mM) = 0.0%
	150215	Dissections	DaGS>UO RNAi			HP(-)=8.3%
						HP(+)=66.7%,8/12
						HP(+) + Kcit(200mM) = 8.3%,1/12
Fig. 14D						
	140131	Dissections	DaGS>UO RNAi			HP(+)=75%,8/12
						HP(+) + Kcit(10mM) = 33.3%,1/12

						HP(+) + Kcit(50mM) = 25.0%,1/12
						HP(+) + Kcit(100mM) = 16..7%,1/12
						HP(+) + Kcit(200mM) = 0.%,0/12
Fig. 15A						
	140905	Dissections	DaGS>UO RNAi			HP(+)=75.00%,8/12
						HP(+)+L-Lys(10µM)=50.0%,6/12
						HP(+)+L-Lys(100µM)=50.0%,6/12
						HP(+)+L-Lys(1000µM)=8.3%,1/12
	150213	Dissections	DaGS>UO RNAi			HP(+)=50.0%,6/12
						HP(+)+L-Lys(10µM)=50%,6/12
						HP(+)+L-Lys(100µM)=33.3%,4/12
						HP(+)+L-Lys(1000µM)=16.7%2/12
	150215	Dissections	DaGS>UO RNAi			HP(+)=66.7%,8/12
						HP(+)+L-Lys(10µM)=33.3%,4/12
						HP(+)+L-Lys(100µM)=8.3%,1/12
						HP(+)+L-Lys(1000µM)=25.0%,3/12
	140905	Dissections	DaGS>UO RNAi			HP(+)=75.00%,8/12
						HP(+)+HCT(10µM)=41.70%,5/12
						HP(+)+HCT(100µM)=50.0%,6/6
						HP(+)+HCT(1000µM)=25.0%,4/12
	150213	Dissections	DaGS>UO RNAi			HP(+)=50.0%,6/12
						HP(+)+HCT(10µM)=58.3%,7/12
						HP(+)+HCT(100µM)=41.7%,5/12
						HP(+)+HCT(1000µM)=33.3%,,4/12
	150215	Dissections	DaGS>UO RNAi			HP(+)=66.7%,9/12
						HP(+)+HCT(10µM)=41.7%,5/12
						HP(+)+HCT(100µM)=25.0%,3/12
						HP(+)+HCT(1000µM)=33.3%,4/12
	140817	Dissections	DaGS>UO RNAi			HP(+)=75.00%,8/12
						HP(+)+MTX(5µM)=0%,0/12
						HP(+)+MTX(50µM)=0%,0/12
						HP(+)+MTX(500µM)=0%,0/12
	140912	Dissections	DaGS>UO RNAi			HP(+)=75.00%,8/12
						HP(+)+MTX(50µM)=41.7%,5/12
						HP(+)+MTX(50µM)=0%,0/12
						HP(+)+MTX(500µM)=0%,0/12
	150213	Dissections	DaGS>UO RNAi			HP(+)=50.0%,6/12
						HP(+)+MTX(50µM)=8.30%,1/12
						HP(+)+MTX(50µM)=16.7%,2/12
						HP(+)+MTX(500µM)=0%,0/12
Fig. 15B						
	140610	Dissections	Da>W1118			HP=0%,0/12
			Da>UO RNAi			HP=33.3%,4/12

						HP+MTX(5µM)=0.0%,1/12
						HP+MTX(50µM)=0.0%,0/12
						HP+MTX(500µM)=0.0%,0/12
	150217	Dissections	Da>W1118			HP=0%,0/12
			Da>UO RNAi			HP=50%,6/12
						HP+MTX(5µM)=16.7%,2/12
						HP+MTX(50µM)=0.0%,0/12
						HP+MTX(500µM)=0.0%,0/12
	150219	Dissections	Da>W1118			HP=0%,0/12
			Da>UO RNAi			HP=66%,7/12
						HP+MTX(5µM)=25.0%,4/12
						HP+MTX(50µM)=0.0%,0/12
						HP+MTX(500µM)=0.0%,0/12
Fig. 16B						
	NP3 Screen	Dissections	DaGS>UO RNAi		HP+A/G(10/10mM)+	
					DMSO(1:50)=66.7%	
					MTX(200µM)=8.3%	
					UAKSI1(200µM)=0.0%,0/6	
					UAKSI2(200µM)=8.3%,1/12	
					UAKSI3(200µM)=10.0%,1/10	
					UAKSI4(200µM)=16.7%,,2/12	
					UAKSI5(200µM)=18.2%,2/11	
					UAKSI6(200µM)=20.0%,2/10	
					UAKSI7(200µM)=20.0%,2/10	
					UAKSE1(200µM)=80.0%,8/10	
					UAKSE2(200µM)=80.0%,8/10	
					UAKSE3(200µM)=81.8%,9/11	
					UAKSE4(200µM)=83.3%,10/12	
					UAKSE5(200µM)=88.9%,8/9	
					UAKSE6(200µM)=90.9%,10/11	